MASTER THESIS

Hydrologic data assimilation for an operational flood forecasting & monitoring system

Analysis of data assimilation schemes through different updated variable types and assimilation window length

Coraline Baud

Swiss Federal Institute of Technology Lausanne - EPFL
Environmental Sciences and Engineering Section - SSIE
Platform of Hydraulic Constructions - PL LCH
Centre de recherche sur l'environnement alpin - CREALP

Supervisor EPFL:
Dr Giovanni De Cesare

Supervisor CREALP:
Dr Theo Baracchini

Lausanne, March, 2022

Acknowledgments

This project was realized in collaboration with the Center for Research on the Alpine Environment (CREALP). I would like to thank the CREALP team for giving me the opportunity to carry out my master project within the company and to discover data assimilation, a field that was still unknown to me. Thanks to the Hydro team, Bastien, Tristan, Javier, who answered my questions and advised me. Special thanks to Theo, who supervised me all along with my project and provided me with a lot of constructive feedback. Thanks also to Giovanni, who supervised this project and welcomed me to the PL-LCH; it was a pleasure to participate in the life of the lab. My thanks also continue to Corinna and Lisa, who reviewed my report. Thanks as well to my family and my boyfriend for their support.

Abstract

Floods in the Rhône River are expected to occur more frequently due to climate change. The sub-catchments of the upper Rhone basin would be more vulnerable to high-intensity flood events. The modeling of hydrological phenomena using process models helps build a robust real-time hydrological forecasting system based on meteorological forecasts to prevent and manage imminent flood risks in Alpine catchments. A complex hydrologic-hydraulic forecasting model for the entire Upper Rhone currently provides automated warnings to a crisis cell of the Canton du Valais and guidance for preventive emptying operations of reservoirs to mitigate flood damage. A transition to a new hydrological model derived from a variant of the well-known HBV model is proposed to improve the performance on flood peaks. Uncertainties may remain in the modeling of complex dynamics such as alpine watersheds. Data assimilation allows to partly overcome these uncertainties by propagating a variables state closer to the flow observations. This study aims to propose different assimilation implementation schemes based on the existing scheme and evaluates which set-up is optimal. Scenario variations include different assimilation window lengths (12h, 24h, 48h and 72h) a different type of updated variable (the soil moisture component or the lower reservoir height). The scenarios evaluation is based on a one-year simulation of the operational system, analyzing the performance in terms of global improvement of the simulation and the hydrological forecast lead time. The study leads to the result that the SL variable brings an important benefit to the hydrological forecasts in a short lead time between 0 and 24h for a 12h assimilation window length. In the case of a flood event, the capability to reach the flood peak is mainly influenced by the previously calibrated parameter set and potentially by the difference in contribution between runoff and base flow related to the flow regime. In case of an event with a high runoff contribution, the SL variable cannot fully compensate for the divergence between the model and the observations either in case of underestimation or overestimation of the flows, which is a limiting factor as it may result in false alarm in the operational system. Nonetheless, the proposed solution contributes to a global system improvement and positively impacts flood monitoring in Valais.

Contents

1 Introduction

Lakes, rivers, waterfalls and glaciers have shaped the mountainous landscape of Switzerland: a complex system that arouses wonder but may turn out to be dangerous. The promiscuity between the danger and the territory constraint makes the cohabitation between humans and nature sometimes challenging. The World Economic Forum identified water-related hazards as being among the highest global risks in terms of impact (WEF, 2020) with damages costs estimated in the order of magnitude of billions CHF per year (WMO, 2021). 20% of the Swiss population lives in flood-prone areas and is therefore susceptible to potential flood damage (FOEN, 2020b). Several important hydrological events have proven the dangerous nature of water, particularly the floods of the Rhône river that occurred in October 2005 in the region of the Canton of Valais in Switzerland.

Due to climate change, natural disasters are expected to occur more frequently and with greater intensity (National Centre for Climate Services, 2018). An elevation of the rain-snow limit and a recrudescence of the episodes of heavy precipitations will consequently participate in an increase of the events intensity and of runoff events (FOEN, 2020a). Furthermore, fast hydrological responses are typical for the most vulnerable zone between 1000 and 2000 m in Alpine catchments characterized by steep slopes, low soil permeability and extensive stream network providing high specific discharge (Weingartner et al., 2003). The modeling of hydrological phenomena through rainfall-runoff models helps to understand the physical processes behind these water dynamics and prevent extensive damage by developing measures to mitigate them.

The Canton of the Valais has set up a hydrological forecasting system for the preventive management and warning of imminent floods based on weather forecasts, a tool to support decisions during emergencies. The real-time operating system is implemented with the free hydrological-hydraulic modeling software (Routing System MINERVE) (J. G. Hernández et al., 2009) developed by the Research Center on Alpine Environment (CREALP). Since 2011, the CREALP continuously operates this complex hydrologic-hydraulic forecasting model for the entire Upper Rhone river basin. It provides automated warnings to a crisis cell of the Canton and guidance for preventive emptying operations of reservoirs to mitigate flood damage. The MINERVE system relies on more than hundred hydro-meteorological field stations covering a domain split into 1440 hydrological models, meteorological forecasts from various providers and numerical atmospheric models, numerous spatial observations (satellites, radars), and an online platform for the timely dissemination of this information. The MINERVE system is among the most advanced solutions flood forecasting and management.

Observation data from hydrological and meteorological measurement stations are used to optimize the parameter states of the process-based GSM-SOCONT[1] model. Despite a large amount of data available, the accurate reproduction of alpine watershed dynamics remains difficult. Errors in parameter or variable states and observation data can persist and affect forecasts. Different data assimilation techniques can be applied to reduce the errors of hydrological models.

[1] Glacier and SnowMelt – SOil CON- Tribution model

1.1 Motivation and Objectives

In the interest of improving the current operational system, CREALP is reviewing the dynamics of the current model by proposing a transition to a new hydrological model derived from a variant of the well-known HBV model (Bergström, 1976). A reliable model is a fundamental element before applying data assimilation, which implies a prior calibration of the parameters set. The calibration is based on new and extensive datasets and enables better modeling of overall dynamics while also improving flood peaks modeling.

Currently, the operational MINERVE system benefits from updating the state variables based on real-time discharge observations at the beginning of each simulation. Thus, data assimilation offers a potential improvement of hydrological forecasts via the propagation of a better set of initial state variables. A. T. Foehn, 2019 implemented a more advanced variant of data assimilation, the Ensemble Kalman Filter (EnKF), which considers input data uncertainties. This method has shown positive results in improving short-term forecasts in a watershed without hydropower influence. The researcher points out that the technique may be too reactive as it is based only on the last flow observation for the initial condition update. However, the forecast's stability is mainly influenced by the quality of the set of model parameters, hence the importance of improving the calibration of the new model.

In this study, we develop a simple and efficient data assimilation algorithm based on the current update scheme of the operational system. The method proposed in this study evaluates different implementation schemes with the new hydrological model by varying the duration and used variable during the data assimilation. Another method combining the initial method with optimizing a cost function will also be discussed. The evaluation will be done over one year of simulation of the operational system. This study will lead to the answer to the following questions:

- How is the modeling performance affected by a transition to a new hydrological model calibrated with recent datasets?
- How can the modeling performance be further improved with a new data assimilation scheme, and what is the optimal setup (e.g., assimilation window length, optimal forecast horizon, updated variable)?

The Upper Rhône river basin system is divided into numerous sub-catchments. This study will consider three sub-watersheds as case studies: the Morge and Sionne for the HBV calibration and the Sionne and Goneri watersheds for the data assimilation.

1.2 Chapters Description

This report consists of the following chapters:

- **Chapter 2** Context and input data: describes the characteristics of the different watersheds studied in terms of geology, external parameters influencing the modeling and the different events during the period under analysis. Available data are also defined.

- **Chapter 3** Theoretical background and literature review: provides an overview of the different hydrological models used in the study and introduces the concept of data assimilation based on the existing literature.
- **Chapter 4** Calibration and validation of hydrologic models: presents and discusses the results of the calibration of the new HBV model in comparison with the original SOCONT model.
- **Chapter 5** Data assimilation: explains the variants of existing and newly implemented data assimilation schemes. Results and discussion are oriented first in a global performance approach, then an analysis at the hydrological event scale is pursued. Finally, a possible outlook of all computed data is presented.
- **Chapter 6** Conclusion: summarizes the insights gained from this study and the various implications for future integrations into the operational system.

2 Context and Input Data

2.1 Studied Watersheds

The studied watersheds are located in the Upper Rhone Basin. They are characterized by steep slopes with a contribution of snow-melt from spring to early autumn. Sionne and Morge watersheds are urbanized in the downstream part, while Goneri is more natural with a rocky composition. The different land uses for each catchment are summarized in Table 1.

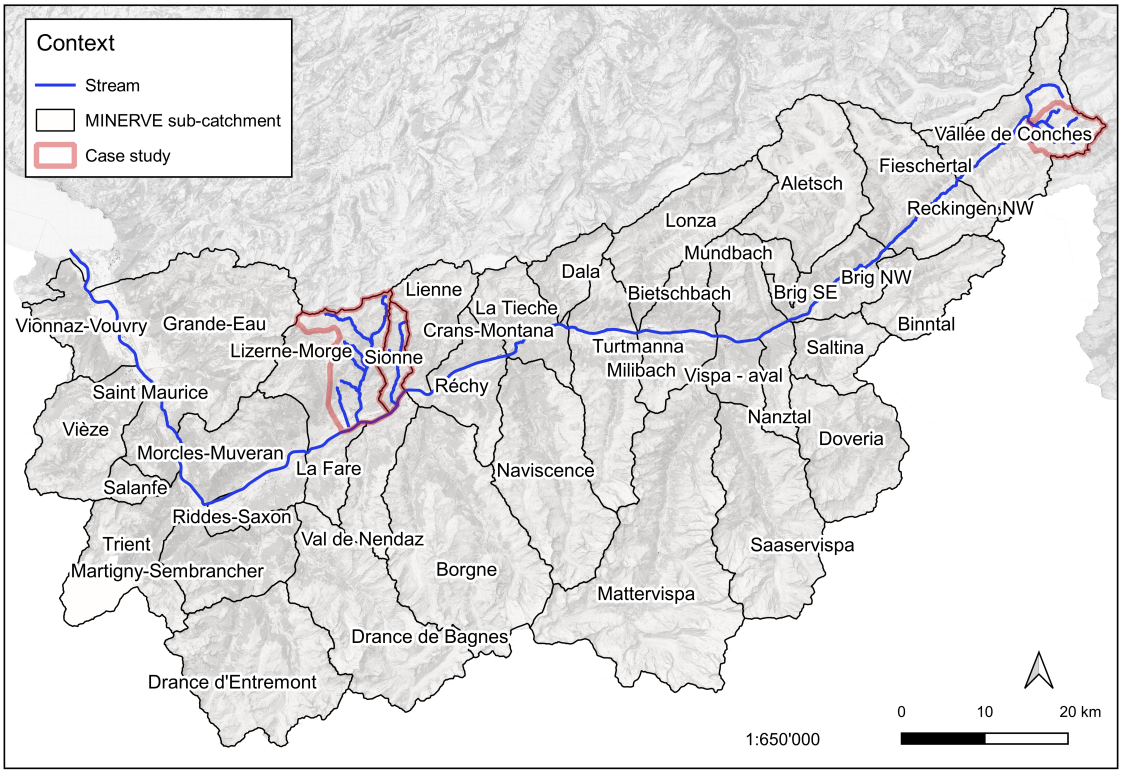

Figure 1 – Geographical context of the studied watersheds : Sionne and Morge in the Central Valais region, and Goneri in the Upper Valais.

2.1.1 Geological Features and Elevation Bands

The operating system is based on a semi-distributed model separated into sub-catchments divided according to their elevation bands. Such a division allows for a better representation of local characteristics linked with meteorological processes induced by altitude variation. The variance of peak flow estimates decreases significantly with an increasing number of subdivisions (Singh and Woolhiser, 2002). Each watershed also remains heterogeneous in terms of both geological and land-use constraints. The latter are represented in Appendix A.2 and A.1.

The hydrological behavior of a watershed is mainly influenced by its geology. Indeed, it impacts the

Table 1 – Land use (data from *swissTLM^{Regio}* and *Hydrological Atlas of Switzerland*)

	Goneri	**Morge**	**Sionne**
Glacier	11%	7%	0%
Wetland	0%	0%	2%
Rock	52%	36%	19%
Unconsolidated rock	10%	29%	12%
Forest	6%	11%	22%
Bushy vegetation	0%	2%	6%
Herbaceous vegetation	21%	2%	12%
Agriculture	0%	6%	11%
Urbanized area	0%	5%	16%

Table 2 – Features of the studied watersheds

	Goneri	**Morge**	**Sionne**
Average elevation [m.a.s.l.]	2383	1574	1577
Elevations interval [m.a.s.l.]	1385 - 3192	476 – 3138	486 – 2878
Average slope	0.53	0.43	0.40
Surface [km^2]	39.6	101.4	31.9
Glacier surface [km^2]	2.8	2.7	-
Average stream slope	0.095	0.098	0.159
Hydraulic pathway [m]	11450	19250	11860
Concentration time [min]	64-93	95-156	54-83
Hourly average flow [m^3/s]	2.5	1.4	0.43

groundwater flow paths, the characteristics of the interface between soil and bedrock and the bedrock impermeability (Vannier et al., 2016). Such differences may affect the water storage capacity and subsurface pathways. The underground in the watersheds of Sionne and Morge is mainly composed of sandstone, clay, limestone and moraine, whereas the underground of the Goneri is composed of a mixture of schist, granite, gneiss and moraine. The upstream part of the Goneri basin can have a specific permeability due to the presence of crystalline fissured rocks. The downstream part belongs to the carboniferous cover of the massif, and they have low permeability.

Differences between soil type and the elevation bands, such as represented in Appendix A.2 may affect the hydrological modeling results, which consider a geological and land use homogenization according to elevation. However, an increase in model scale has the effect of transforming non-stationary into stationary hydrological processes and allows the use of the same parameters set for each elevation band (Singh and Woolhiser, 2002).

2.1.2 Bisse Irrigation Network

The bisses constitute part of the Valaisan heritage. They are irrigation canals used traditionally to irrigate vineyards since the 19^{th} century and more recently for tourism purposes (Reynard, 2002).

Currently, 80% of the irrigated areas (vineyards and meadows) are irrigated through bisses in the Valais. This channels network is particularly dense in the Sionne and Morge catchment areas (Figure 2). Water generally flows in the bisses from April to October; nevertheless, some bisses are perennial. According to the information obtained from the Bisses museum[2], several bisses influence the Sionne and Morge watersheds.

Bisses of the Sionne watershed:

- Bitailla (Municipality of Arbaz and Ayent) irrigates Arbaz and Ayent and withdraws about 3/4 of the water of the Sionne at the Bitailla point (Figure 2). The water intake is operational all year round.
- Bisse of Grimisuat (Municipality of Grimisuat).
- Bisse of Lentine (Municipality of Savièse) supplies water to the lake and the bisse of Montorge.
- Bisse of Sion (Oiken, Municipality of Sion) brings water from the Lienne to the Sionne. It was built for this purpose around 1903.
- Bisses of the Tsampé and the Bordzi used to take water from the Fontanys springs and currently takes water from a tunnel connected with the Sionne.

For the Morge:

- Bisse of Tsandra (Municipality of Conthey).
- Bisse of Déjore (Municipality of Savièse) supplied by a tunnel from the Morge.

The locations of the main above-mentioned water intakes and discharges are represented in Figure 2. Some of the hydraulic infrastructures are also illustrated in Appendix A.4. These complex withdrawals may significantly influence the downstream river flow and are not considered in the model. For the locations mentioned, the more upstream elevation bands have a 3/4 of this flow diverted into the Bitailla bisse. Precise discharges are challenging to estimate since the water rights remain assigned using quota (such as 1/4, 1/2, 3/4 quota) without specific discharge from the municipality or a consortium and seem to be managed partially with manual operation rules, resulting in a potential decrease in the quality of the calibration for low discharges.

2.2 Input Data

2.2.1 Temperature and Precipitation Data

Rain and temperature gauges data from SwissMetNet (SMN) are used as input data for the real-time operating system in RS MINERVE (RSM) and are represented in Figure 3. The spatial distribution

[2] G. Morard, personal communication, February 11, 2022

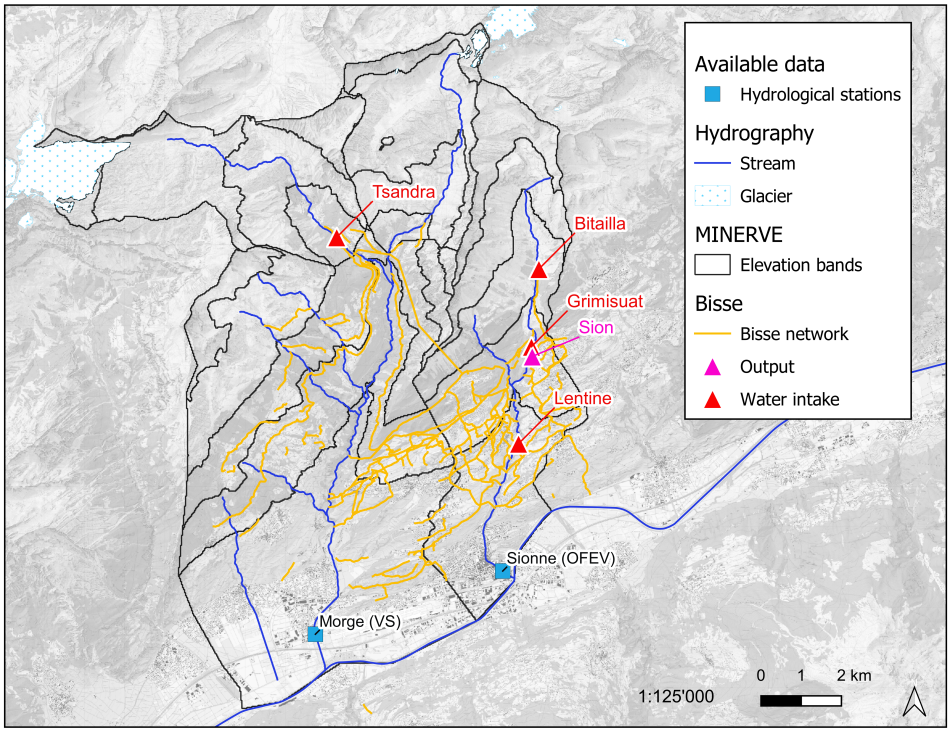

Figure 2 – Bisse network in Sionne and Morge catchment with localisation of identified water intakes and outlet of the Bisse of Sion

of the data is then implemented using virtual stations for each elevation band. A weighting of the available meteorological stations based on the nearest distance is then calculated for each virtual station. The stations that have an influence on the Sionne and Morge are Anzère, Tsanfleuron, Sion, Montana, Derborence and Les Collons. And for the Goneri, they are the stations Ulrichen, Grimsel Hospitz, Blinnen, Robièi, Guttannen, Gaescherneralp and Airolo. Next, precipitation data are computed based on an inverse distance weighting interpolation from the observed stations values. Each watershed considers a constant adiabatic lapse rate calculated during the calibration process.

Sionne and Goneri watersheds are not well covered by the SMN network by not having measuring stations within the distribution area. Meteorological conditions in the Alps can be very local. A lack of network density will result in smoothing the spatial interpolation and not reproducing local dynamics. Spatial variability of precipitation could not be accurately reproduced, especially during a rapid heavy rain event or during winter thermal inversion. A combined method using rain gauges network and weather radar data showed better performance than the unique use of rain gauges; however, low radar visibility areas have still uncertain performance (A. Foehn et al., 2018), however this method is not used in the operational system.

The SMN network provides the operating system with raw data in real-time with a ten-minute time-step. These data is used in the calibration and data assimilation parts. Their availability for the Sionne and Morge watersheds is illustrated in Appendix A.5.

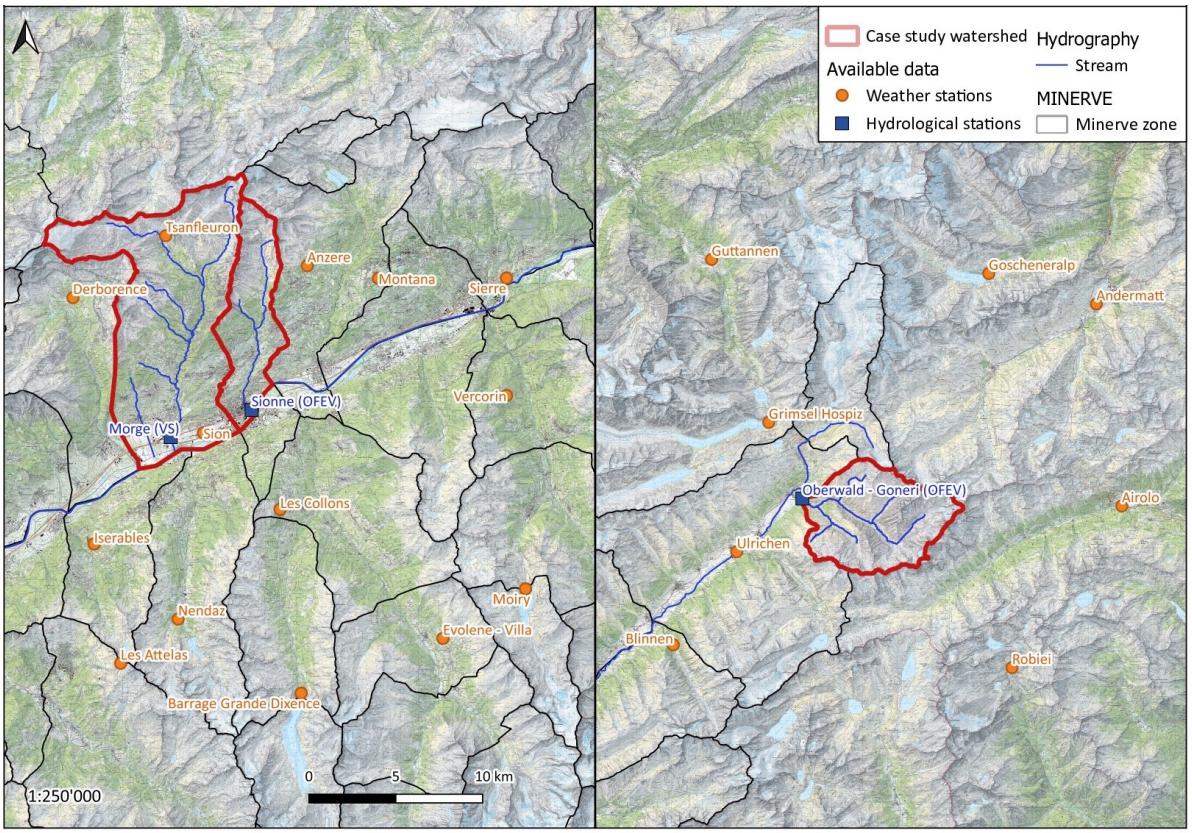

Figure 3 – Meteorological stations for spatial interpolation and flow measuring stations

2.2.2 Discharge Data

The observation flow data come from the Swiss hydrographic network of the Federal Office for the Environment (FOEN) (for the Sionne and the Goneri) and the hydrographic network of the canton of Valais (RHcVS) (for the Morge). The two different types of stations do not benefit from the same financial means. Thus, the cantonal stations do not have such rigorous quality controls as the federal ones. The Morge measuring station is recent, with data available since 2014, but CREALP has validated only data from the year 2017. Regarding the FOEN hydrological stations, the data have been approved until July 2021 in November 2021 and have been available since 1991 for the Goneri and 2006 for the Sionne. The location of the studied stations is illustrated in Figure 3. As for the meteorological data, raw data with a resolution of 10 minutes are downloaded for the calibration and during the data assimilation.

2.3 Studied Hydrological events

Concerning the calibration and the data assimilation part, this report will study various events separately for each basin (Table 3). In view of the events considered, a more extended analysis period (from October 1, 2020 to October 1, 2021) has been studied to quantify the global performance of the

different data assimilation schemes. The illustration of these discharges is given in the Appendix A.6.

Table 3 – Features of the studied events

	Goneri	Morge	Sionne
Period	1 - 6.10.21	12 - 17.07.21	12 - 17.07.21
Hourly peak flow [m^3/s]	118.5	23.9	4.4
Estimated return period [years]	>100	5	9

2.3.1 October 2020

The event ran from October 2 at 8 a.m. to October 3 at 8 a.m. During this time, precipitation totals between 100 and 250 mm were recorded. Figure 4 shows extreme rainfall events with a return period between 30 and 50 years in the Upper Valais region. Consequently, discharge records were reached at the Goneri measuring station.

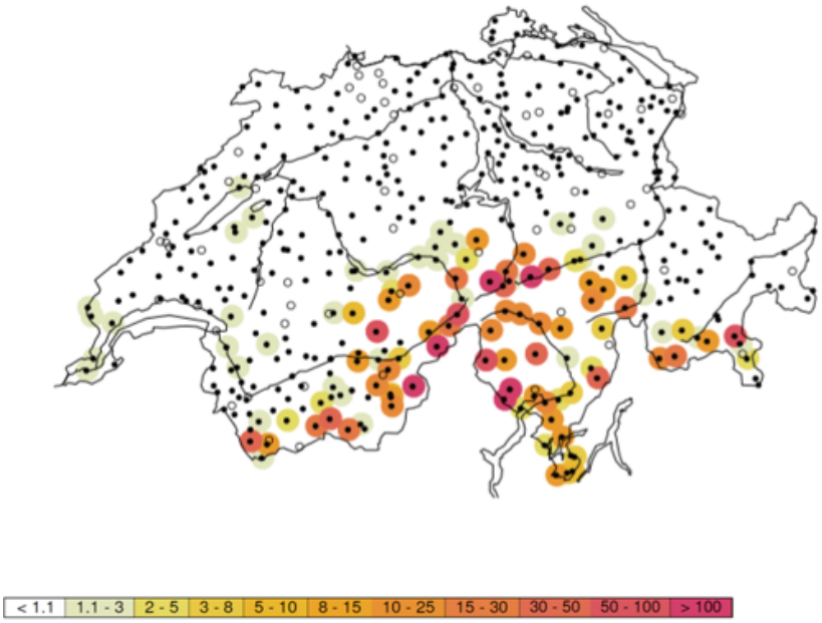

Figure 4 – Return period for one day of precipitation on October 2, 2020 : from October 2 at 8 a.m. to October 3 at 8 a.m. (“MeteoSwiss”, 2021)

2.3.2 July 2021

The situation in July 2021 is characterized by above-average precipitation totals in the preceding months and by a month of June with relatively high temperatures, which led to intense snowmelt and soil saturation. Further precipitation with an accumulation of more than 150mm from July 12 to 15 in the Morge and Sionne catchment areas (Figure 5) caused small floods.

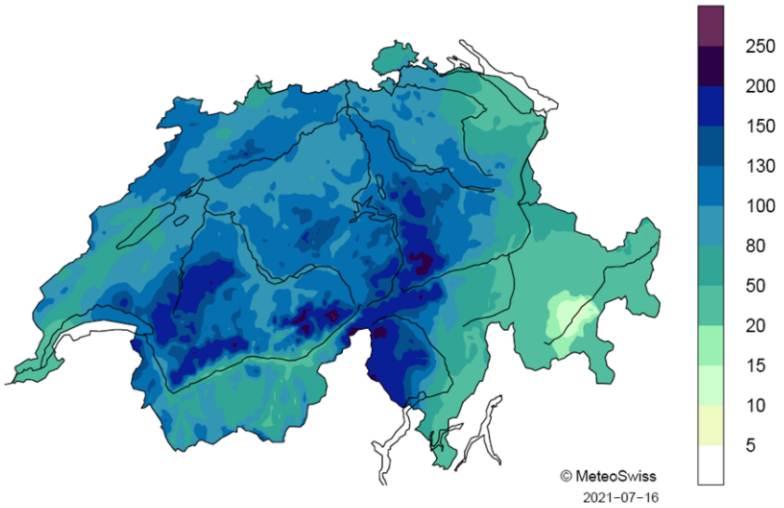

Figure 5 – Precipitation totals from July 12 to 15, 2021 (“MeteoSwiss”, 2021)

3 Theoretical Background and Literature Review

3.1 Hydrological Models

This report introduces two different hydrological models: SOCONT and HBVS. Each of them has a snow compartment and a soil/surface compartment for the non-glacial part of the sub-catchment. The models are then completed by a GSM model for the modeling of the glacier part.

3.1.1 SOCONT

The partial SOCONT model is shown in Figure 6. From the temperature (T) and precipitation (P) data, the Snow-SD model supplies the infiltration reservoir (i_{inf} in the model GR3) and the surface runoff (i_{Net} in the model SWMM) with equivalent precipitation (P_{eq}). The outflow is generated by adding the linear response of the infiltration reservoir and the nonlinear response of the surface runoff model. Further detailed equations can be found in the RS MINERVE technical report (Garcia Hernández et al., 2020).

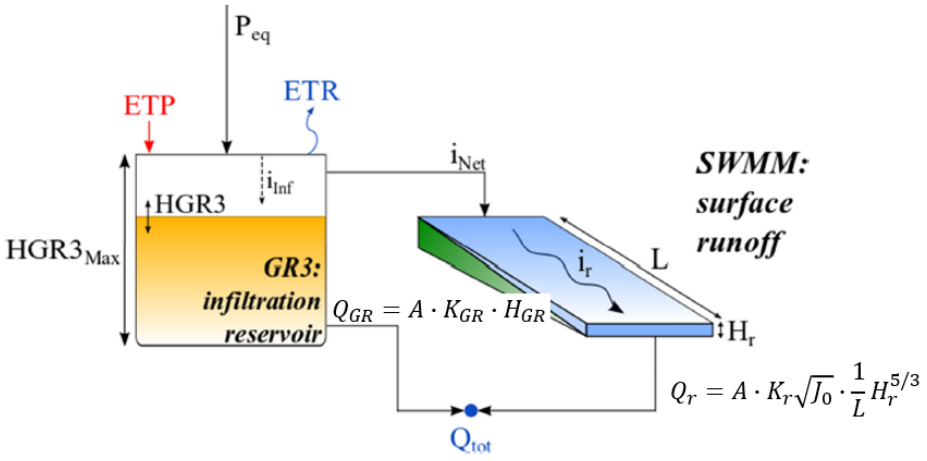

with
- A: Surface $[L^2]$
- H_{GR3}: Level in the infiltration reservoir $[L]$
- K_{GR3}: Release coefficient of infiltration reservoir $[1/s]$
- K_r: Strickler coefficient $[L^{1/3}/T]$
- L: Length of the plane $[L]$
- J_0: Runoff slope $[L]$
- H_r: Runoff water level downstream of the surface $[m]$
- ETP: Potential evapotranspiration $[L/T]$
- ETR: Real evapotranspiration $[L/T]$

Figure 6 – SOCONT model

3.1.2 HBVS

As for the SOCONT model, the equivalent precipitation P_{eq} is generated by the Snow-SD model. The outflow results from cascading compartments through the humidity reservoir and the addition of lower and upper soil storage reservoirs.

HBV model (HBV-92) was developed by Bergström, 1976 and different variants of the HBV model were developed over the years. Further investigations from the CREALP have shown that both SOCONT and HBV-92 models may not fully reproduce some peak flows, especially during noteworthy events. A change in the response function with a non-linear drainage equation from the soil reservoir (reflected by the addition of the parameter AlphaU) allowed a better high flow performance and a more dynamic response of the watershed without compromising the overall simulation results(Lindström et al., 1997). Furthermore, the combination of the superficial and intermediate outflow equations prevents an overparameterization in the upper reservoir. The changes reduce the number of the parameters to be calibrated, thus a decrease in the model complexity. The new HBV from the HBV-96 variant was named HBVS in RS MINERVE and is currently implemented in RS MINERVE only for the operational system in the Upper Valais, while the other regions are running with the SOCONT model. The HBVS model has already demonstrated better performance in the Upper Valais watersheds by CREALP.

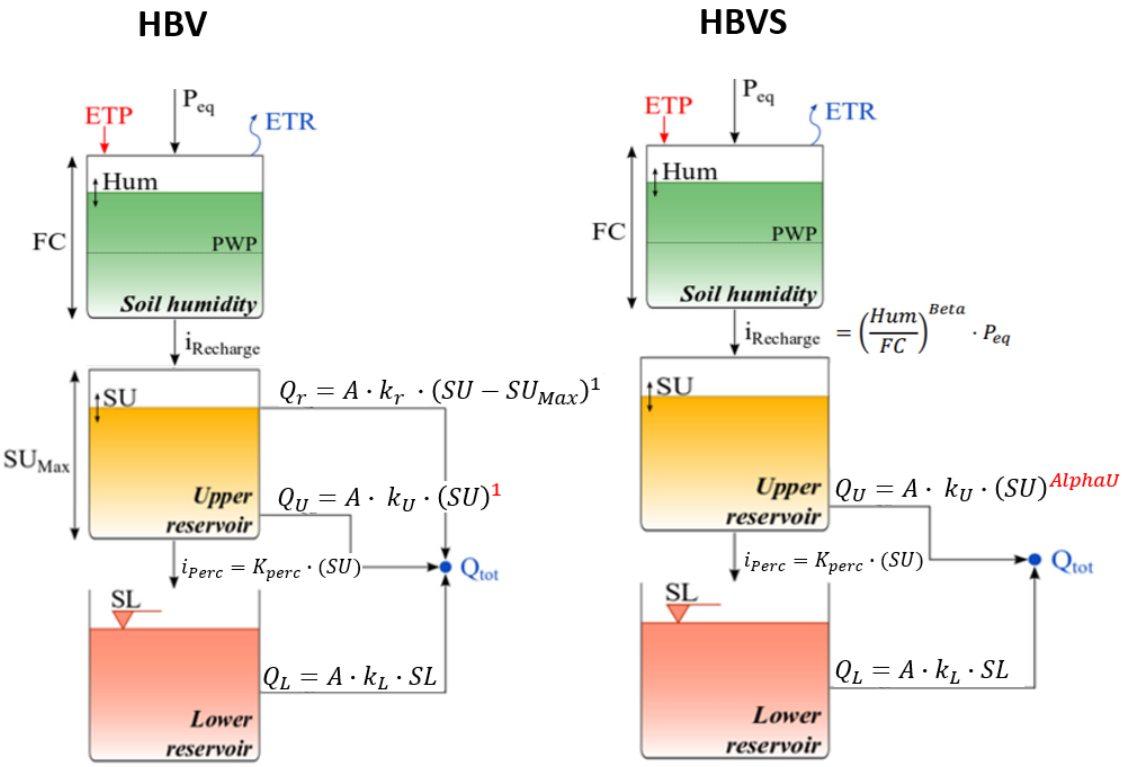

with
A: Surface $[L^2]$
Hum: Humidity $[L]$
SU: Level in the upper reservoir $[L]$
SL: Level in the lower reservoir $[L]$
k_r: Near surface flow storage coefficient $[1/T]$
k_u: Interflow storage coefficient $[1/T]$
k_l: Baseflow storage coefficient $[1/T]$
k_{Perc}: Percolation storage coefficient $[1/T]$
FC: Maximum soil storage capacity $[L]$
β: Model parameter (shape coefficient) $[-]$
αU: Non-linearity shape coefficient $[-]$

Figure 7 – HBV and HBVS model

3.2 Hydrological Data Assimilation

Flow prediction is necessary for proper emergency management. Minimizing and quantifying uncertainties can reduce potential false alarms and guide authorities in decision-making. Uncertainty in hydrological prediction may derive from errors in the models parameters or from the initial conditions used as well as from external inputs (meteorological data) (Y. Liu et al., 2012; Park and Xu, 2017). Assimilation of in-situ data such as discharge, soil moisture or snow height and assimilation of

remote sensing data have been developed to improve the predictions by considering the different sources of uncertainties. Such a method assumes that by enhancing past model states based on fresh observations during a certain assimilation window, the model will better represent the future evolution of the data. Figure 8 illustrates the process with a schematic view. Several methods have been developed to meet the needs of hydrological forecasting, a selection will presented in the next chapter.

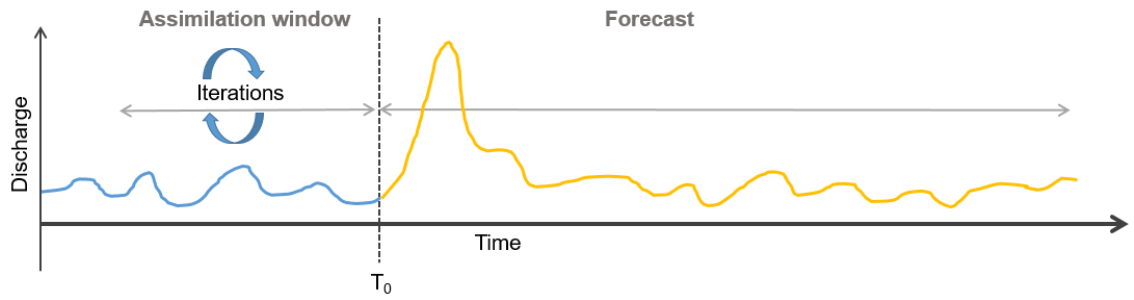

Figure 8 – Schematic illustration of the data assimilation process: blue curve represents the observations and the yellow curve the hydrological forecasts

3.2.1 Bayesian and Variational Data Assimilation

The first technique, called variational data assimilation (VAR), seeks to minimize a cost function between the observations and the simulated values by updating the initial conditions of the state variables within a given assimilation time window. Nudging is a continuous data assimilation method, which adds a term proportional to the difference between the observations and the model simulation to state variables (Lei and Hacker, 2015). The operational system is based on this method. Those techniques do not provide an indication of the uncertainties of the estimated predictions and limit the additional value of the updated variables in case of an emergency decision-making process (Abbaszadeh et al., 2019). The most widely used approach in the field of hydrology is the Kalman type Filter, more precisely the Ensemble Kalman Filter (EnKF) version (Y. Liu et al., 2012). The method consists of generating an updated state of variables based on weighting factors by means of the state and the observation error covariance from a Gaussian errors statistics assumption. Forecast simulations will then be updated by propagating the quantified error. This method was developed to cope with non-linearity processes such as hydrodynamics. However, this technique does not provide a way to derive the prior distribution of the simulated variables. Several variants have been developed to counter this restriction: the Extended Kalman Filter (EKF) that linearizes the model before finding the error covariance matrix and uses a set of model trajectories (Evensen, 1994). The latter remains easy to implement and has already proven its robustness in many cases (Javaheri et al., 2018; Da Ros and Borga, 1997; Reichle et al., 2002; Samuel et al., 2019). Nevertheless, the linearization of the model can result to instability when the degree of nonlinearity increases and requires a high computational cost.

An alternative to the EnKF is the Particle Filter (PF) which relies as well on an ensemble of multiple model trajectories but does not apply the Gaussian assumption of the state variables and parameters distribution (Abbaszadeh et al., 2018). However, this technique has the disadvantage of requiring many particles to correctly evaluate the distribution of the variables (high computational cost) and produce a degeneracy of the particles. Convergence to an imbalanced particles weighting may occur; hence the particles cannot reproduce the optimal forecast simulation. Some advanced algorithms allow to counter this problem by resampling or filtering the particles.

Hence, two schools of thought emerge in data assimilation techniques. The first can be identified as techniques that create a probabilistic estimate of the parameters and variables space, including its uncertainties (EKF, EnKF, PF). The second (VAR, Nudging) is a more traditional technique that optimizes the simulation according to the observations and also has the advantage of being less demanding in terms of computation. F. Hernández and Liang, 2017 suggested a hybrid algorithm that targets non-linear high-resolution problems and may overcome the disadvantages of both schools of thought.

3.2.2 Choice of the Assimilation Window Length

The performance of the model will depend in part on the choice of the assimilation window length. Its selection shall be made accurately and should not be left to chance. It can be defined in terms of ensemble size (i.e., depending on the number of input data) or in terms of duration (time).

Many recent studies have performed a systematic analysis of the assimilation size to optimize its performance (F. Hernández and Liang, 2017; Rafieeinasab et al., 2014). The choice can also be made for computational reasons, where Dumedah and Coulibaly, 2013 fixed 60 data points to perform the assimilation and others concluded at an ensemble size of 1000. The experiments of F. Hernández and Liang, 2017 suggests that "there is an ideal duration of the assimilation time step that is dependent on the case study under consideration and the spatiotemporal resolution of the corresponding model application."

The length would also depend on the type of assimilation method used: PF method seems to require a larger sample size than other filtering methods; the ensemble size would also increase with the number of state variables (Fan et al., 2017). Whereas for the VAR method, the assimilation window length should be comparable (Seo et al., 2003; Lee et al., 2011) or longer (S. Liu et al., 2012) than the runoff time scale from the most upstream area to the watershed outlet so that the memory of the system is well-reflected.

In this last perspective and considering the time of concentration of the studied watersheds (see Table 2), the assimilation time should be about 2h. This duration seems to be very short, given that the sample size would amount to only 10 data points. A risk of over-fitting is not to be excluded in this case, and Jordan, 2007 recommended a minimum 12h window length. In order to analyze the performance according to the window length, the duration of 12h, 24h, 48h, 72h will be tested.

4 Calibration and validation of hydrological models

4.1 Method

Catchment dynamics may change over the years, maybe due to natural processes or due to human interventions (Pathiraja et al., 2016). A new calibration with recent observations fills in some of the non-stationarity of the parameter set and allows to update the changes in dynamics within the watershed.

The calibration method has been developed by the CREALP (Baracchini, 2021). Five sequential steps are necessary to calibrate the Sionne and Morge HBVS/GSM models based on flow observation and SMN data as input. The first four steps consist of an automatic calibration with RSM software, each using the default parameters of the RSM SCE-UA[3] algorithm with a weighting of the performance indicators of 2 for Nash, 1 for Pearson, 0.75 for Relative Volume Bias (RVB)[4]. Finally, the last step is performed manually on the peak flows: its increase allows better capture of the flood peaks even if the global performance is slightly lower. In summary, the methodology includes:

1. Preliminary calibration with global parameters including the temperature gradient for the Virtual Stations.
2. Calibration of the snow part of the GSM and HBVS models.
3. Calibration of the soil parameters of the HBVS model.
4. Fine-tuning calibration on parameters with significant impacts on the simulation results
5. Manual calibration of AlphaU$_{HBVS}$ parameter (see Chapter 3.1.2) to obtain better peak modeling, potentially at the cost of the "normal" dynamics".

The calibration is started with the most recent data available. Next, a validation period will be necessary to evaluate the performance of the model outside the calibration data range. The SOCONT model was calibrated for all sub-catchments of a defined region simultaneously. The performance results of the HBVS model and the SOCONT operational model will be analyzed on a global performance and in view of flood peaks during the above-mentioned event (see Chapter 2.3).

4.2 Sionne

An alpine nival regime characterizes the Sionne River. The flood peaks are mainly linked to precipitations which can be very localized. There is a daily variation of about 100 l/s in the low water period and about 1000l/s in the summer period. Anthropogenic influences have been highlighted, particularly the use of the bisses as irrigation channels; however, their exact influence remains difficult

[3] Shuffled Complex Evolution – University of Arizona (Duan et al., 1993)
[4] see Appendix B.1 for detailed indicators calculation

to estimate. The measuring station of the Sionne is located just upstream of the junction with the Rhône. The discharge data are available from 2006, and no major event has been recorded so far.

Results and discussion

The table of initial and calibrated parameters is shown in Appendix B.2, and the graphs are presented in Figure 11.

The initial SOCONT model overestimates observed discharges along the year. The seasonal dynamics related to snowmelt are also not well represented. Peak floods are not reached even if too much water is observed over the entire system.

Following the calibration with the HBVS model, the NSE, Pearson, and RVB indicators[5] are significantly improved with a score of 0.77, 0.89 and 0.072, respectively (Table 4). Despite such an enhancement, an NSE lower than 0.8 remains very poor. However, modeling is generally more difficult for such small basin areas due to heterogeneity. In contrast, the validation period has a very low score which can be explained by the lack of available data. In fact, between the years 2006 and 2011, only data from the stations of Montana and Sion are available.

Table 4 – Evaluation of the NSE, Pearson and RVB indicators following the calibration of the HBVS model for the Sionne watershed in comparison to SOCONT model.

Calibration period: 2011-2021
Validation period: 2006-2011

	SOCONT	**HBVS**		
	2011-2021	Calibration	Manual	Validation
NSE	0.31	0.78	0.77	0.25
Pearson	0.8	0.89	0.89	0.74
RVB	0.6	0.092	0.072	-0.488

A slight increase in the temperature gradient is observed compared to the initial version, i.e., from -0.0054 to -0.0048 °C/m. Overall, the seasonal dynamics are better represented with better modeling of snow-melt. The model does not reproduce daily variations, but the simulated flow is centered on the observations. The base flow is also better modeled and has a significant contribution to the total flow (Figure 9).

Some peaks are challenging to model because they are conducive to very rapid flood peaks that even the HBVS model is not able to reproduce well. They are potentially related to very localized precipitation events (such as the storm north of the city of Sion in August 2018 with an observed discharge of 6 m^3/s). The distribution of state variables indicates that precipitation contributions are more critical on the upstream altitude bands, with a distribution of the moisture variable directed towards the maximum holding capacity. The downstream elevation bands have a more uniform distribution of the Hum variable and could explain a restricted reproduction of rapid high peaks such as observed in August 2018 in this sector.

[5] see Appendix B.1 for detailed formulas

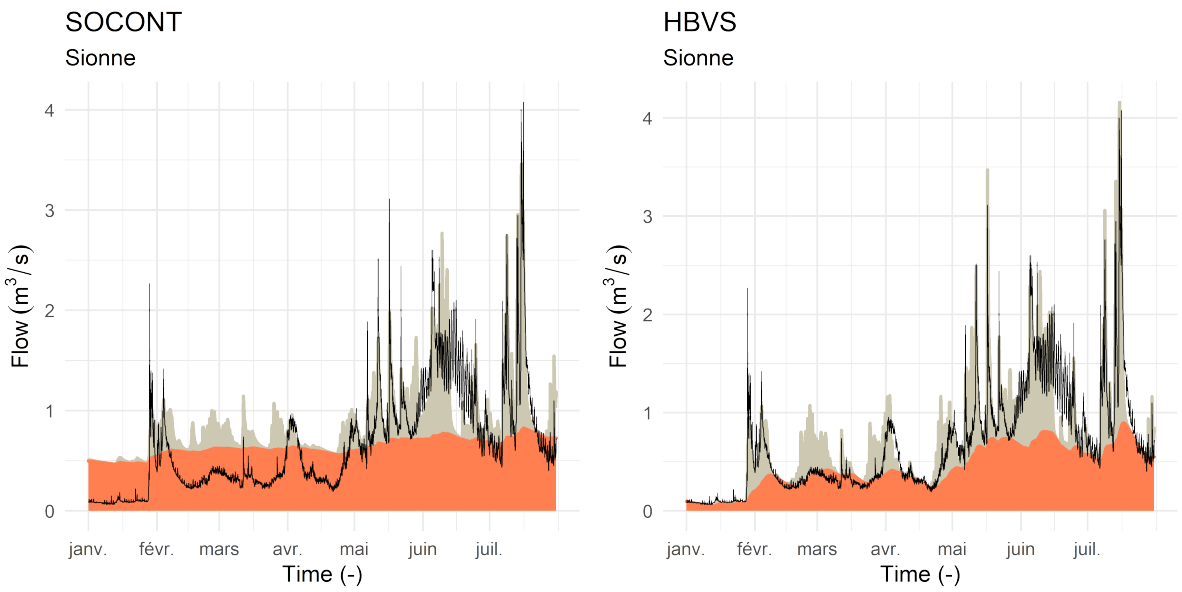

Figure 9 – Comparison of base flow contribution (coral color) and runoff contribution (gray color) between the HBVS and SOCONT model for the Sionne.

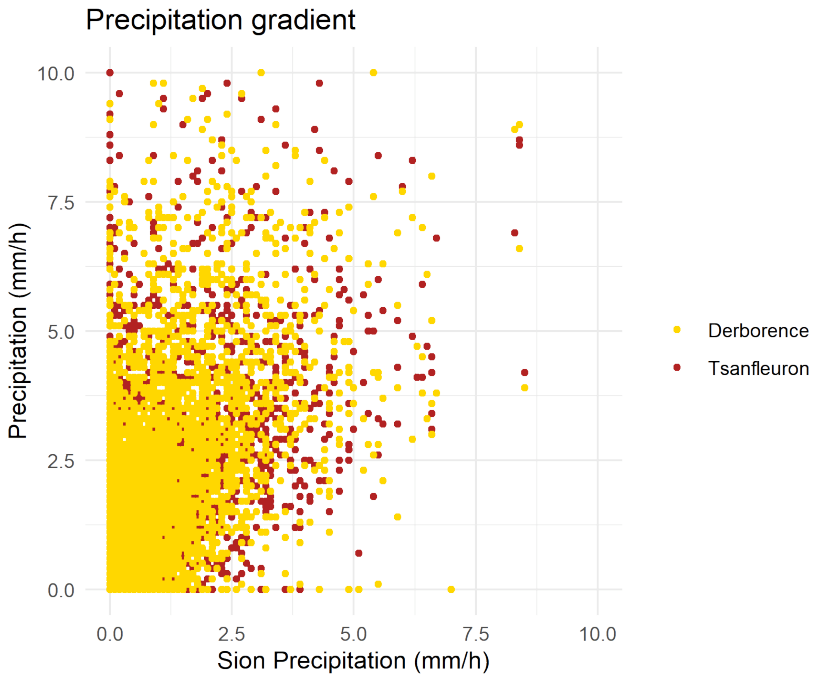

Figure 10 – Precipitation gradient between the downstream Sion weather station and upstream Derborence/Tsanfleuron weather station.

The discharge of the upstream elevation bands is particularly influenced by the withdrawals from the Bitailla Bisse. By decreasing only the contribution of the upstream elevation bands by 10%, the NSE score can be increased by 2%. This excessive water input has a potential influence on the ability of the model to dynamize the variations during a flood flow. The results of the calibration parameters show that the Sionne has a high retention capacity of the soil compartment with a FC of 0.49 m; thus, the influence of precipitation is attenuated. This result is physically feasible because the Sionne watershed is characterized by a more permeable geology. This basin does not have a weather station in its perimeter. It is, therefore, difficult to say whether the overestimation comes from unmodelled water withdrawals or whether the spatial interpolation of meteorological data does not represent the physical reality. Contrary to the SOCONT model, the HBVS model can mathematically compensate for input uncertainties and, therefore, focus the dynamism on the observations. Concerning the July 2021 event, both models are relatively similar, and both do not succeed in reaching the peak floods (Figure 11c).

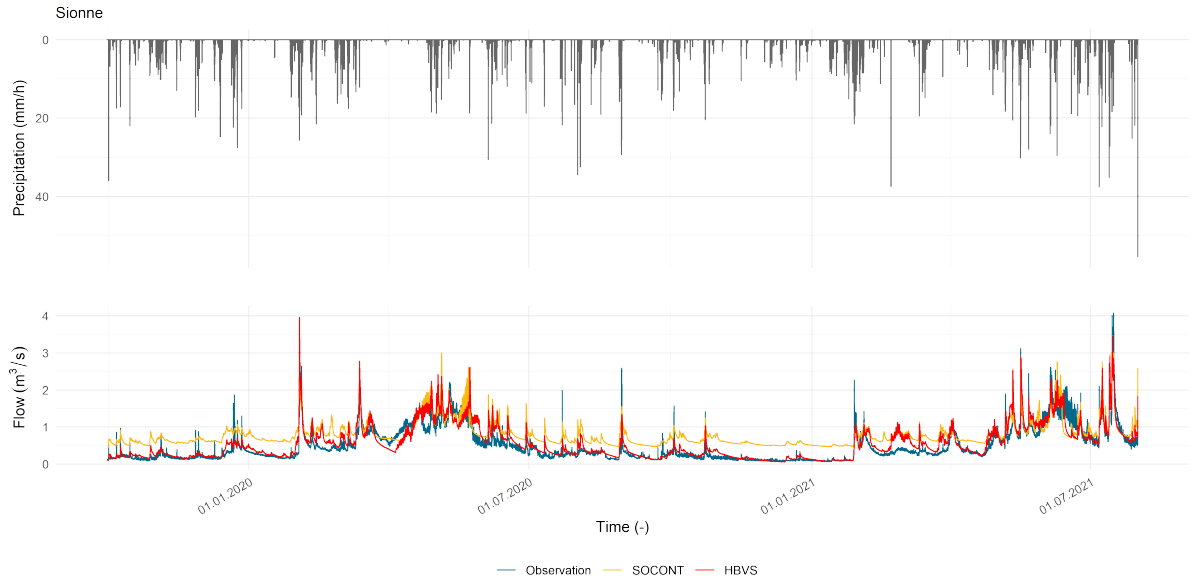

(a)

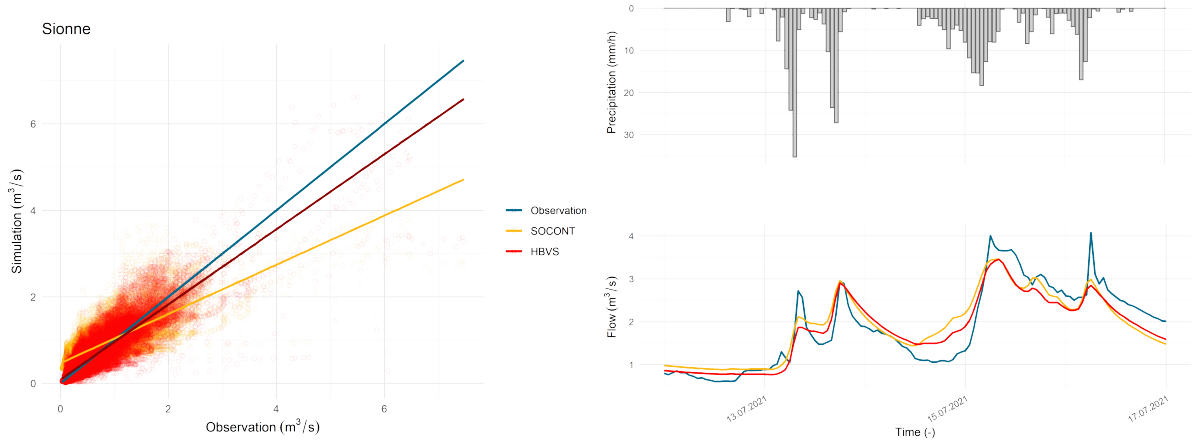

(b) (c)

Figure 11 – Evaluation of the HBVS model compared to the SOCONT model for the Sionne watershed: a) global view during the period from October 1, 2019 to August 1, 2021 with precipitation modeled by RS MINERVE, b) scatter-plot of the results with their linear regression, c) smaller scale view on the July 2021 event with precipitation modeled by RS MINERVE.

4.3 Morge

Influenced by the Tsanfleuron glacier and a smaller glacier situated in the East of the watershed, the Morge is further characterized by a nivo-glacial regime. The flow measurement station is also located upstream of the confluence with the Rhône. At this location, the riverbed is channelized with a consequent width, which implies a thin water layer and may have consequences on the low flow estimations. Moreover, the field visit allows identifying the presence of relatively medium-size boulders in the stream, which can also influence the water level if they are carried.

The SOCONT model of the Morge has the same type of errors as the one of the Sionne, too high base flows, a too large modeled volume and a significant contribution of flows from the Tsanfleuron glacier. The flood peaks are partially reached.

Results and discussion

A first calibration converged to a solution with a temperature gradient of -0.0077 °C/m. The consequence of such a gradient was an accumulation of snow in the glaciers, and thus no snow-melt was simulated by the model. It is then likely that the model generates too much water, and the calibration tends to a solution to compensate for this effect by eliminating the influence of the glacier part. This solution also includes parameters that converge at the edge of their range limit, which suggests that the model fails to reproduce the physics of the watershed. In such watershed types, precipitation comes mainly from mountain tops, and the spatial interpolation might propagate the precipitation too far downstream (Figure 10). However, by adding the precipitation coefficient to the automatic calibration, the latter tends to increase the contribution of rainfall (115%), which rejects the hypothesis that the accumulation would be linked to an erroneous spatial interpolation.

By analyzing the temperature gradient between the observations of the stations of Sion/Tsanfleuron and Sion/Derborence, an average gradient of -0.0047 °C/m is observed, well above the gradient determined during the calibration. It was then decided to define the temperature gradient with the observations of the stations and not to calibrate it. The results of the calibration are reasonable and converge rather towards a decrease of the snow-melt contribution (12) without calibrated parameters at interval edges.

Table 5 – Evaluation of the NSE, Pearson and RVB indicators following the calibration of the HBVS model for the Goneri watershed in comparison to SOCONT model.

Calibration period: 2017-2021
Validation period: 2014-2017

	SOCONT	**HBVS**		
	2017-2021	Calibration	Manual	Validation
NSE	-0.033	0.77	0.75	0.573
Pearson	0.7	0.88	0.87	0.810
RVB	1.2	0.00	0.06	0.157

The table of initial and calibrated parameters is provided in Appendix B.2, the graphs are presented in Figure 13.The results of the HBVS model are appreciable, with more centered flows, but the daily

dynamics do not manage to be reproduced. Peak floods are not systematically reached.

Following the calibration with the HBVS model, the NSE, Pearson, and RVB indicators are significantly improved with a score of 0.76, 0.88 and 0.065, respectively (Table 5). For the validation period, a significant decrease is observe which is probably related to the poor quality of the flow observation data. However, the calibration score is again rather low given that the network of meteorological measuring stations contains two measuring stations in this watershed. This may be partly explained by the relatively short calibration period and the gap in precipitation data from Tsanfleuron, a station with a significant weighting, during May and June 2021. The Tsanfleuron glacier is located in a karst region. A study has shown that the Tsanfleuron glacier recharges the aquifer via shallow holes 3 km downstream the glacier (Gremaud et al., 2009). Thus, part of the outflow from the glacier is diverted from the stream, and this could explain the decrease of the glacier contribution in the results. Considering the July 2021 event, the flood peaks are not entirely reached but an improvement compared to SOCONT is discernible. The HBVS model may compensate for the uncertainties related to the low flows and the karst influence by a decrease in the response of the SU reservoir.

At the end of 2021, a new measuring station at the Sanetsch Hotel was installed (about 5-km downstream from the glacier). New calibrations in several years could be helpful to model the karstic influence in the river better and have more robust parameters.

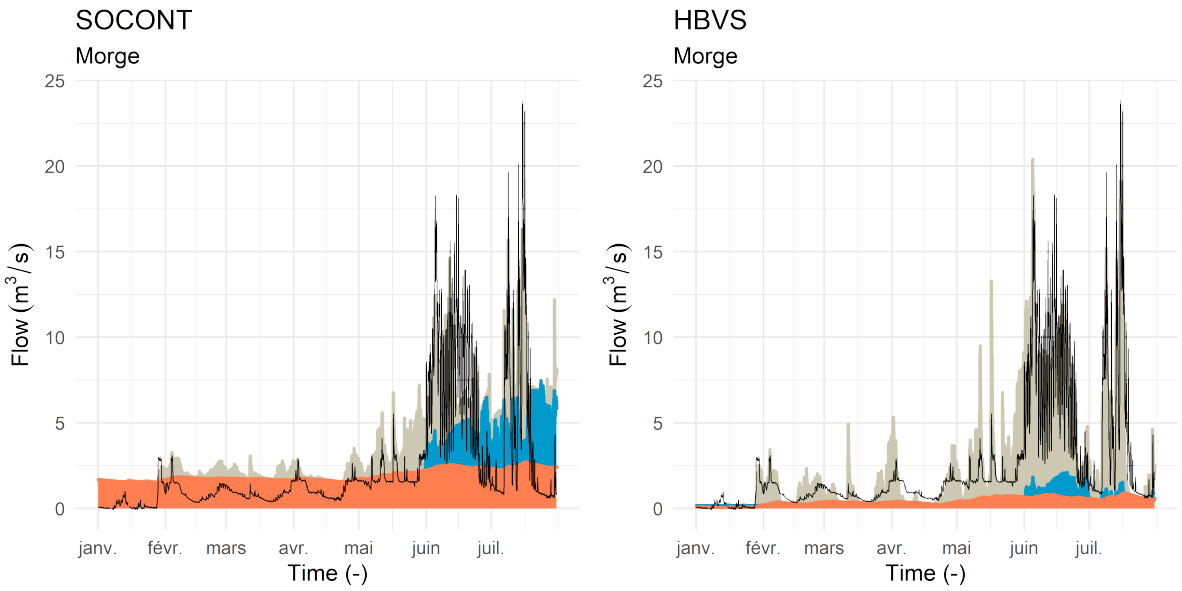

Figure 12 – Comparison of base flow contribution (coral color), runoff flow (gray color) and glacier flow (blue color) between the HBVS and SOCONT model for the Morge.

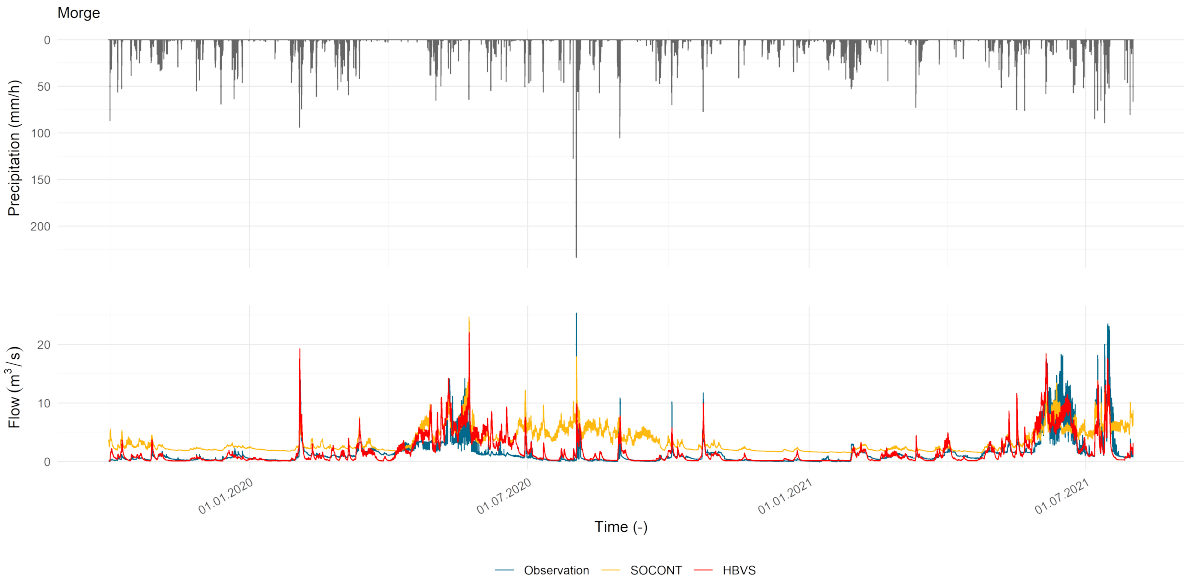

(a)

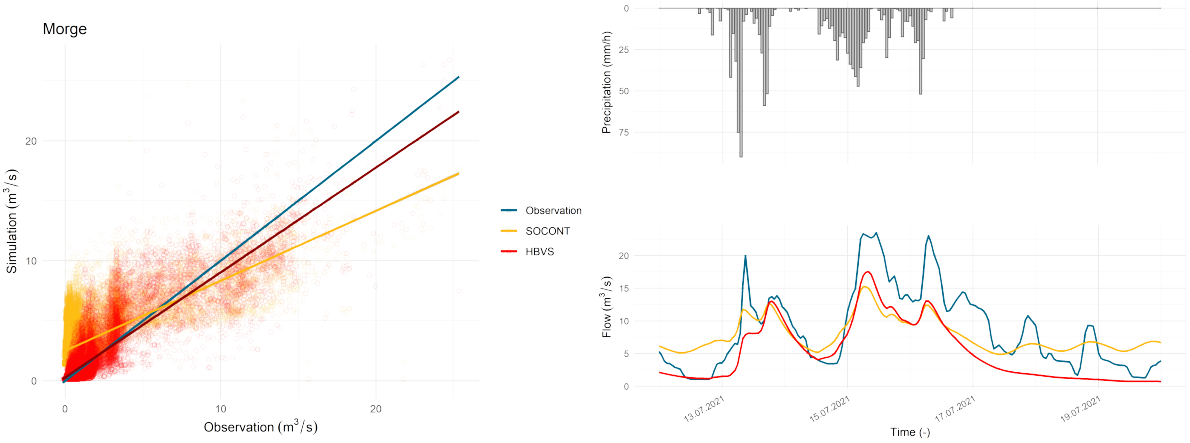

(b) (c)

Figure 13 – Evaluation of the HBVS model compared to the SOCONT model for the Morge watershed: a) global view during the period from October 1, 2019 to August 1, 2021 with precipitation modeled by RS MINERVE, b) scatter-plot of the results with their linear regression, c) smaller scale view on the July 2021 event with precipitation modeled by RS MINERVE.

4.4 Goneri

The calibration and analysis of the Goneri were performed by CREALP before the FOEN discharge validation, and their various findings are summarized in this section. The Goneri is subject to a particular dynamic with many peaks characterized by a glacial-nival regime, which made it difficult to model. According to the CREALP, at first, the SOCONT model performed well and represented the daily dynamics adequately.

FOEN furnishes real-time observation data for the operational system, and several years after, the service validated the data. Usually, this validation does not introduce much change, but this is not the case for the Goneri here. The validated flows show a marked difference in the peak flood of October 2020, with a peak at 118.5 m^3/s instead of 89 m^3/s previously registered. There is much uncertainty on the exact value of the peak because the FOEN validation introduced a significant amount of water in the hourly peak by linearizing the peak rise from the measured values. The new calibration of the HBVS model allowed us to better model the peak flood of this event by reaching a discharge of 75 m^3/s against an initial discharge of 30m^3/s. The additional flow provided by the calibration during this event comes mainly from the increase of the temperature gradient (from -0.0054 to -0.0039 °C/m) and the addition of the non-linearity parameter (alphaU). However, the FC and Beta parameters reached the bounds imposed by the calibration. Although a small FC may be consistent with low permeability geology in the Goneri watershed, this type of behavior may indicate that the model is struggling to reproduce the physical variability of the observed system with the parameters defined in the calibration or that the spatial interpolation is not representative of the meteorological conditions of the basin. The new calibration also influenced the outflow of the glacier part by increasing it during the summer period and on the runoff flow by raising all the peak flows (Figure 14).

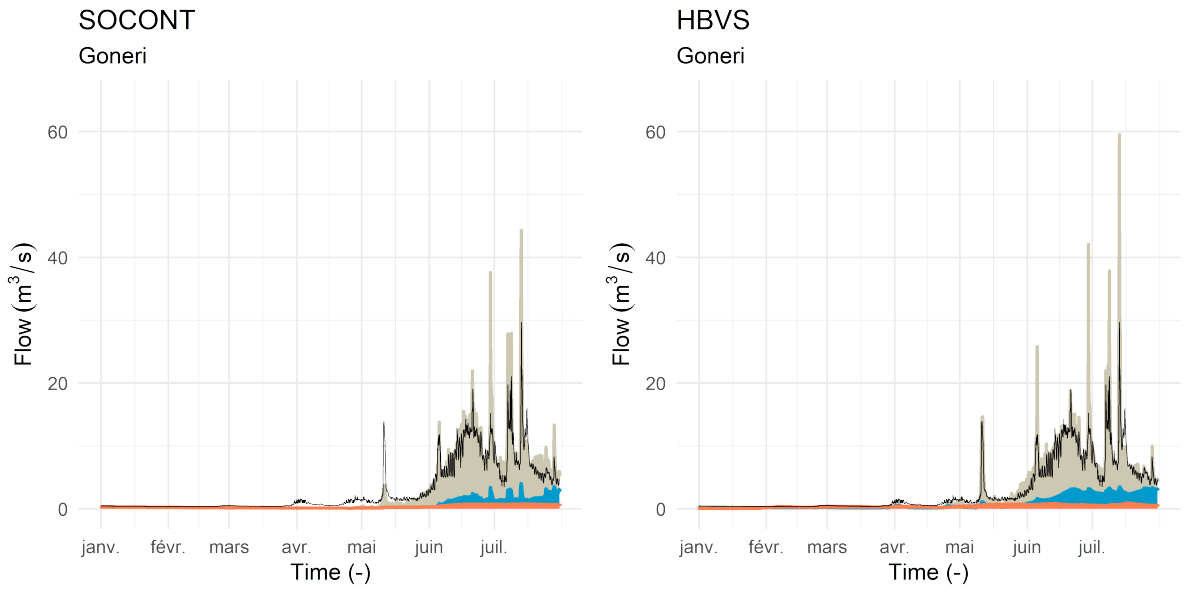

Figure 14 – Comparison of base flow contribution (coral color), runoff flow (gray color) and glacier flow (color blue) between the HBVS and SOCONT model for the Goneri.

5 Data Assimilation

5.1 Material and Methods

5.1.1 Actual Data Assimilation in the Operational Flood Forecasting System of the Upper Rhone River Catchment

The real-time operational system calculates the hydrological forecasts every 2 hours based on the meteorological forecasts furnished by MeteoSwiss. With the aim of not considering the uncertainties of weather forecasts and to perceive the real effect of assimilation on hydrological forecasts, observational data were used as a basis for analysis instead of the MeteoSwiss forecasts. Two types of forecasts are provided by the operational system: a control and an update version[6].

Control (CTRL)

This version is based only on resetting the initial conditions 24 hours before the time t_0. It consists of a continuous simulation of the calibrated model, often called open-loop simulation in the literature, using the variable states at t_0 to predict the hydrological forecasts.

SOCONT - Volume Based Update

The method is established by updating the initial soil saturation conditions H_{GR3} from the SOCONT model (see Figure 6) to obtain modeling as close as possible to the 24 hours of flow observation before the forecast. The initial conditions of the variable H_{GR3} are iteratively updated using a change scale factor ζ based on the relative volume bias (RVB) between the observed and simulated flows. The change scale factor ζ is calculated with the following equation :

$$\zeta = \begin{cases} 2.5 & \text{if RVB} \leq \text{-0.6} \\ \dfrac{1}{\text{RVB} + 1} & \text{if - 0.6} < \text{RVB} < 4 \\ 0.2 & \text{if RVB} \geq 4 \end{cases} . \tag{1}$$

$$\text{with} \qquad \text{RVB} = \frac{Vol_{obs} - Vol_{sim}}{Vol_{sim}} \tag{2}$$

The initial soil saturation conditions H_{GR3} is updated for each iteration if the RVB is higher then 0.05 with : $H_{GR3_{i+1}} = \zeta \cdot H_{GR3_i}$

The iterations proceed until the convergence threshold of the RVB (0.01) or the max number of iterations (10) are reached. The optimization is thus saved in the initial conditions used for the next time-step. This approach can be considered as an evolutionary data assimilation since it does not start again from the simulation control but from the previous UPDT time-step results.

[6] This section is inspired by chapter 5.2 from the Thesis of Alain Foehn (A. T. Foehn, 2019)

5.1.2 Implementation of the HBVS Model in the Operational System

The same technique as the assimilation for the SOCONT model is used, which consists in updating the initial conditions of one of the variables of the soil compartments applying the same change scale factor ζ (Equation 1). Here, several scenarios of variable updates are considered [7]: the variable *Hum* (Humidity variable in the first soil reservoir) and the variable *SL* (Level in the lower reservoir). Each of these scenarios is analyzed for the data assimilation window variants, i.e., 12, 24, 48, and 72 hours as mentioned in Chapter 3.2.2.

A second assimilation method to mitigate against the effects of an inaccurate update (method OF)

Using the RVB indicator alone in the assimilation could lead to a false optimum. In fact, if the flow variations are important in the assimilation window, the optimum solution for convergence would be a straight line in the middle of these flow oscillations, thus, it could strongly alter long-term forecasts. A second method was then implemented in an attempt to overcome this issue. It is a method that combines the volume base update and a VAR method, and that seeks to optimize a cost function based on the objective function (OF) used during the calibration process in the RSM software[8]. The addition of the Pearson coefficient with the indicator RVB allows considering the correlation between observed and simulated flows, which prevents the daily oscillations not to being reproduced. The convergence threshold had to be lowered (0.002) compared to the initial volume base update because the use of the Pearson indicator leads to a very stable OF function. The weighting of the indicators has a significant impact on the number of iterations and the update performance. The choice of weighting turned to a balanced solution between computational cost and volume optimization.

The method also includes the scaling factor ξ. The first two iterations are derived from simulated and observed volume differences. The iterations proceed then by incrementing the initial conditions by 10% according to the results of the previous OF function until convergence or the maximal number of iteration, which has been increased to 300, is reached. It is expressed in the following way :

$$\text{Iteration 1: } \xi = 1 + |\text{RVB}_0| \tag{3}$$

$$\text{Iteration 2: } \xi = 1 - |\text{RVB}_0| \qquad \text{if } \text{OF}_1 \text{ ł } \text{OF}_0$$

$$\xi_i = \begin{cases} 1.1 & \text{if } \text{OF}_{i-1} \geq \text{OF}_{i-2} \\ 0.9 & \text{else} \end{cases} . \tag{4}$$

$$\text{with} \quad \text{OF} = \text{Pearson} \cdot 0.6 - |\text{RVB}| \cdot 0.4 \tag{5}$$

The initial conditions of the iterations obtaining the best cost function are loaded for the calculation of the forecasts and are held for the next time step.

[7] (detailed scheme of the HBVS model in Figure 7)
[8] Garcia Hernández et al., 2020

5.2 Experimental Set-up

All calculations are performed in the R programming language (R Core Team, 2019) and are based on the existing routine of the operational system. The modifications made were in the data acquisition (more precisely, the change of the weather forecast data into observation data), in the implementation of the HBVS model and, finally, in the second data assimilation method.

For each of the studied scenarios, depending on the window assimilation length and the type of updated variables, the operating system was launched for a period of one year (From October 1, 2020, to October 1, 2021). A total of 16 scenarios per watershed are studied for each data assimilation method.

The global performance with the NSE indicator for each watershed (Goneri and Sionne) is assessed during the mentioned period. A more qualitative and visual evaluation on the scale of an event (referred in Chapter 2.3) is also brought into the analysis.

The different scenario terminologies presented in this chapter can be summarized as follows:

- **RVB**: Initial data assimilation method which relies on the RVB indicator
- **OF**: Second data assimilation method which relies on the maximization of the objective function
- **CTRL**: Open-loop HBVS model
- **Hum**: Update of initial Hum variable during the assimilation (HBVS)
- **SL**: Update of initial SL variable during the assimilation (HBVS)
- **SOCONT**: Update of the initial H_{GR3} during the existing assimilation (SOCONT)

The variant SU was at the beginning studied as well, but for the sake of simplicity, those results are not presented here as improvements were not significant. An example with the assimilation of the SU variable is illustrated in the Appendix C.1.

5.3 Global Performance Assessment

5.3.1 Results

- **Improved simulation thanks to data assimilation**

The performance of the data assimilation is reported for the RVB method and the OF method, respectively in Figures 15 and 16. The upper figure shows the evolution of the RMSE for each different assimilation duration according to the updated variable in comparison with the CTRL simulation without data assimilation. The lower figure shows the global performance using the NSE indicator

of each scenario in comparison with the control simulation and the initial SOCONT assimilation. Numerical results are presented in Table 6.

Table 6 – Numerical results of NSE indicators and mean RMSE for each of the implemented scenarios according to each catchment.

Method RVB

SIO		CTRL	12-h		24-h		48-h		72-h	
			Hum	SL	Hum	SL	Hum	SL	Hum	SL
	NSE	0.79	0.910	0.954	0.907	0.938	0.903	0.922	0.895	0.908
	RMSE	0.15	0.081	0.061	0.087	0.077	0.095	0.091	0.100	0.102
GON		CTRL	12-h		24-h		48-h		72-h	
			Hum	SL	Hum	SL	Hum	SL	Hum	SL
	NSE	0.81	0.958	0.859	0.942	0.846	0.900	0.845	0.878	0.845
	RMSE	0.84	0.462	0.389	0.512	0.451	0.610	0.536	0.698	0.607

Method OF

SIO		CTRL	12-h		24-h		48-h		72-h	
			Hum	SL	Hum	SL	Hum	SL	Hum	SL
	NSE	0.79	0.629	0.950	0.685	0.938	0.824	0.920	0.862	0.909
	RMSE	0.15	0.191	0.061	0.161	0.076	0.132	0.092	0.122	0.102
GON		CTRL	12-h		24-h		48-h		72-h	
			Hum	SL	Hum	SL	Hum	SL	Hum	SL
	NSE	0.81	0.369	0.920	0.465	0.911	0.568	0.892	0.631	0.880
	RMSE	0.84	1.490	0.355	1.379	0.415	1.387	0.463	1.400	0.550

Method RVB

In general, the RVB method allows an improvement of the simulation for all the considered scenarios (Figure 15) compared to the CTRL simulation. The assimilation is very efficient for the Sionne watershed and results in a distribution converging towards 0 for the RVB indicator and a decrease in the RSME (Figure 15a). The improvement is more remarkable for the SL variant than the Hum variant. Moreover, we observe an optimization of the RVB indicator by increasing the assimilation length for the Hum variant, while the SL variant shows the opposite effect with the RMSE indicator. Regarding the overall NSE scores (Figure 15b), the Hum variant appears to be constant with assimilation length. On the other hand, we observe an increase in NSE with decreasing length. The scenario that outperforms the SOCONT method for the Sionne is the SL variant with a 12-hour assimilation window.

Concerning the distribution of RMSE and RVB scores for the Goneri watershed, similar behaviors stand out for each of the updated variables: a constant distribution for each RVB and RMSE for all assimilation windows (Figure 15a). However, the SL variant converges to a distribution more centered towards the optimum value than the Hum variant. On a global performance, the Hum variant presents the best results (Figure 15b). An increase in NSE score is observed with the decrease of the assimilation length, and each of these assimilation lengths outperforms the initial SOCONT update. The SL variant, in the meantime, is somewhat consistent for any scenario but with a better

score for 12-hour assimilation.

Method OF

In terms of convergence of the objective function, the enhancement fluctuates according to the assimilated length and the type of variable with a tighter distribution for the Sionne watershed (Figure 16a). However, there is an improvement in comparison to the control version. The evaluation is more revealing in the RVB indicators where the range of the distribution clusters on the zero value for the SL variant. We also note a decrease in the range of distribution of the RVB with an increase in the duration of assimilation for the Hum variant. While for the SL variant, the RSME performance increases when the assimilation time is shorter.

Regarding the Goneri watershed, an apparent improvement is observed for each of the indicators RVB, RMSE and the objective function for the SL variant. Minimal variation is observed in terms of the difference in assimilation length. As for the Sionne watershed, the values of RVB are concentrated at their optimum for the SL variant.

An opposite trend can be identified between the two updated variables: for the SL variant, a decrease in assimilation window length induces a better NSE score, whereas, for the Hum variant, an increase in assimilation duration leads to a better NSE score (Figure 16b). Contrary to the RVB method, the scenarios of the Hum variant implemented with the OF method are deteriorating the simulation lower than the CTRL one on global NSE indicators, except for the 48 and 72h variants for the Sionne watershed. However, the benefits of the SL variant for a 12-hour assimilation time are significant for both watersheds and have a better NSE score than the initial SOCONT assimilation method. This scenario outperforms previous results obtained with the RVB method.

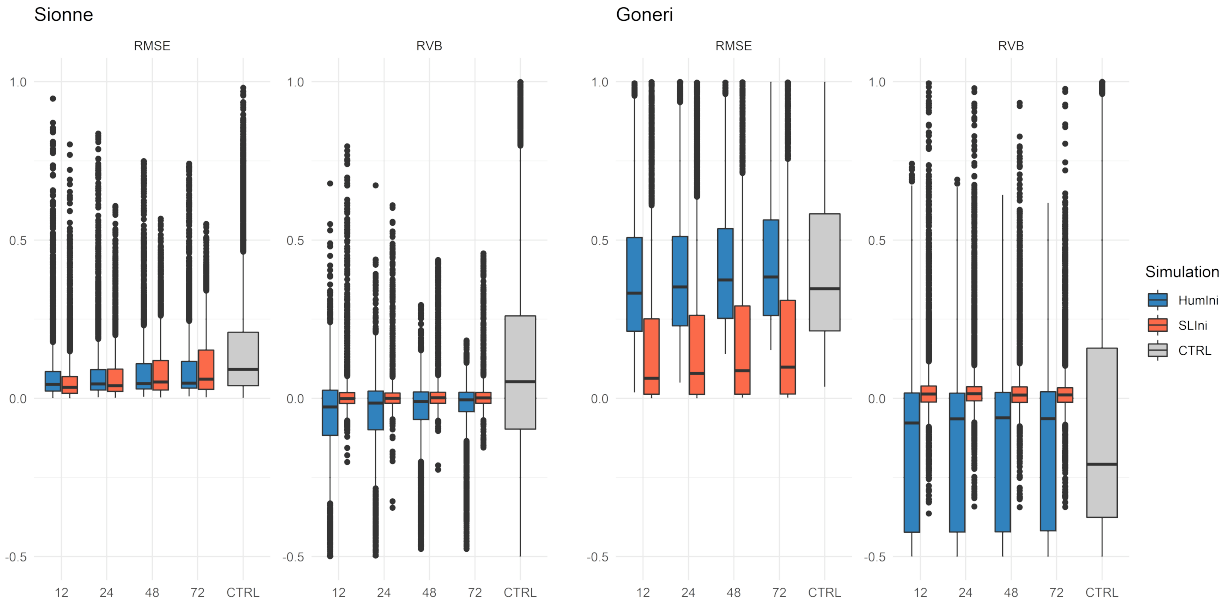

(a)

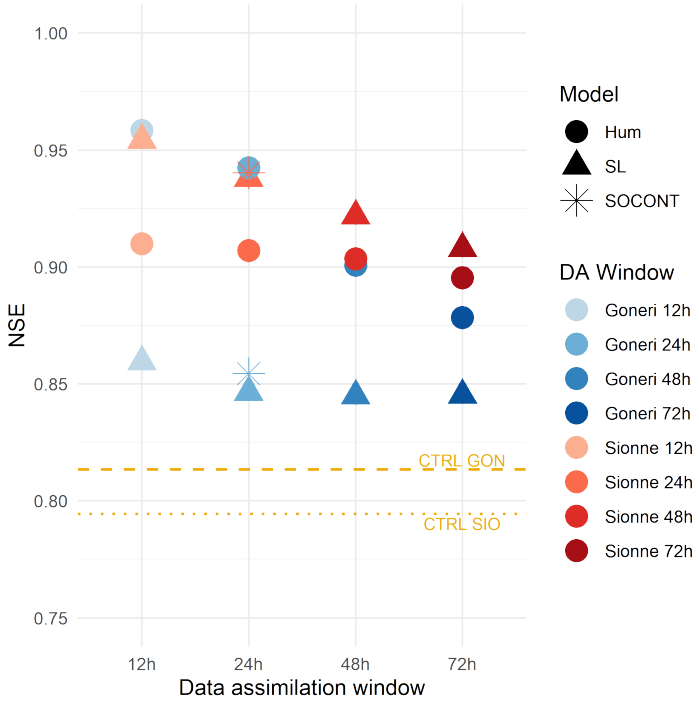

(b)

Figure 15 – Evaluation of the RVB method according to the type of the implementation scheme: a) Results of the distribution of RVB and RMSE indicators, b) illustration of NSE scores compared to the current data assimilation (SOCONT) and CTRL simulation (yellow).

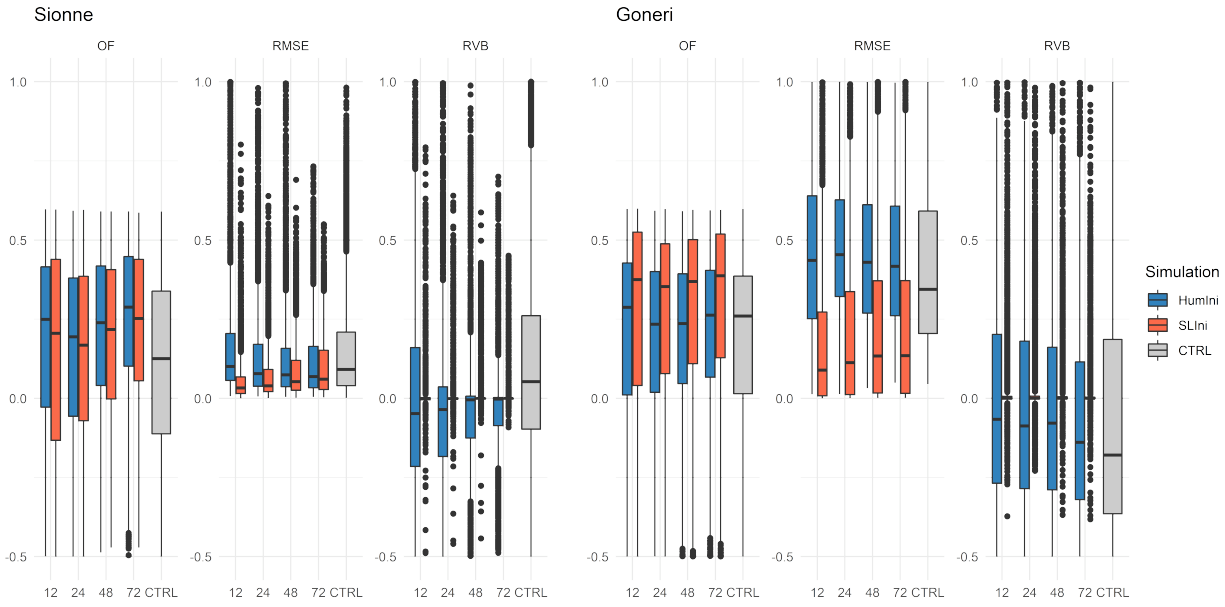

(a)

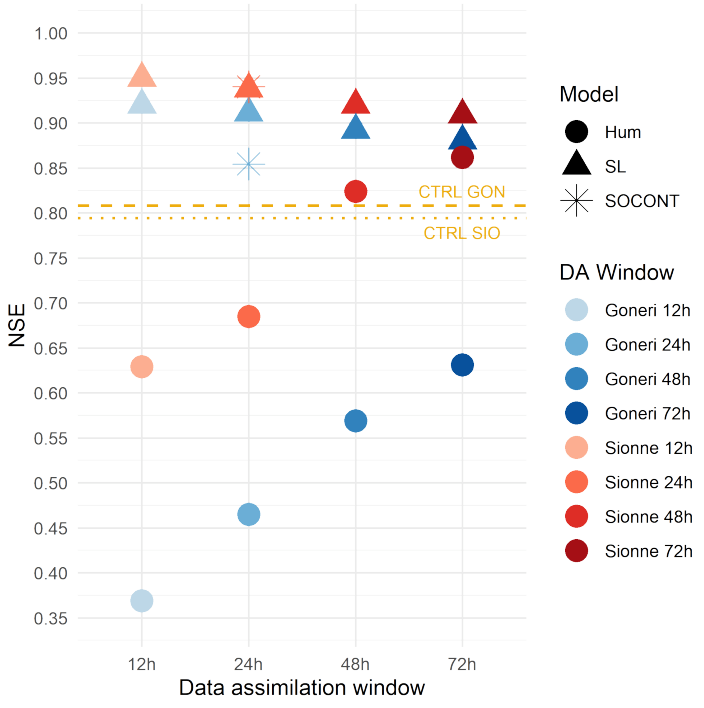

(b)

Figure 16 – Evaluation of the OF method according to the type of the implementation scheme: a) Results of the distribution of the objtective function (OF), RVB and RMSE indicators, b) illustration of NSE scores compared to the current data assimilation (SOCONT) and CTRL simulation (yellow).

- **Effects on forecasts**

In a second step, the propagation of the data assimilation allows assessing on which time horizon the effects of the improvement are optimal.The forecasts are then split into several horizons between 0-24h, 24h-48h and finally 48-120h (Figures 17 and 18), for the method OF and RVB, respectively.

The spread of the assimilation with the Hum variant worsens the hydrological forecasts by revealing a lower NSE score than the CTRL simulation for both watersheds when using the OF Method. The results of the SL variant bring to light that this approach leads to improved forecasts. An assimilation length of 12 hours allows the best progress in a shorter time horizon, i.e., between 0 and 24h, while using a 24-hour assimilation window achieves better results in the longer term.

The RVB method reveals that for Sionne, the assimilation with the Hum variable does not improve the forecasts compared to the CTRL version. It should be noted that a longer assimilation period has better performance for this variable. The results of the SL variant suggest a greater improvement for a shorter assimilation period. As for Goneri, better short-term predictions are achieved for shorter assimilation, whereas a longer assimilation period with the SL variable will be preferred for a long-term improvement. It should also be mentioned that all forecasts are very close to the control simulation results.

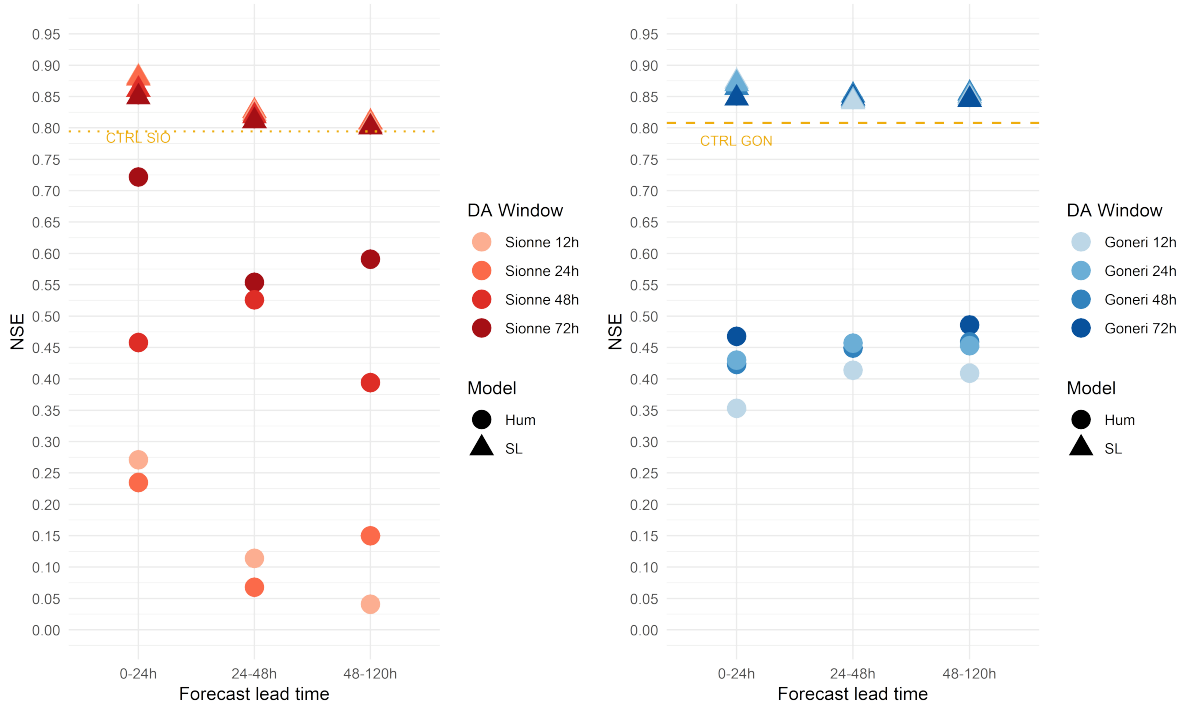

Figure 17 – Method OF: Results of the global indicator (NSE) for the different DA window during the forecast

Table 7 – Numerical results of NSE indicators along forecast horizon for each of the implemented scenarios according to each catchment using method OF.

Method OF									
SIO		12h		24h		48h		72h	
		Hum	SL	Hum	SL	Hum	SL	Hum	SL
	CTRL	0.79							
	0-24h	0.271	0.881	0.235	0.879	0.458	0.861	0.722	0.849
	24-48h	0.114	0.823	0.068	0.827	0.526	0.819	0.554	0.811
	48-120h	0.041	0.804	0.15	0.809	0.394	0.804	0.591	0.801
GON		12h		24h		48h		72h	
		Hum	SL	Hum	SL	Hum	SL	Hum	SL
	CTRL	0.81							
	0-24h	0.353	0.874	0.430	0.870	0.420	0.864	0.468	0.847
	24-48h	0.414	0.841	0.457	0.844	0.449	0.852	0.457	0.847
	48-120h	0.409	0.848	0.453	0.851	0.459	0.855	0.486	0.845

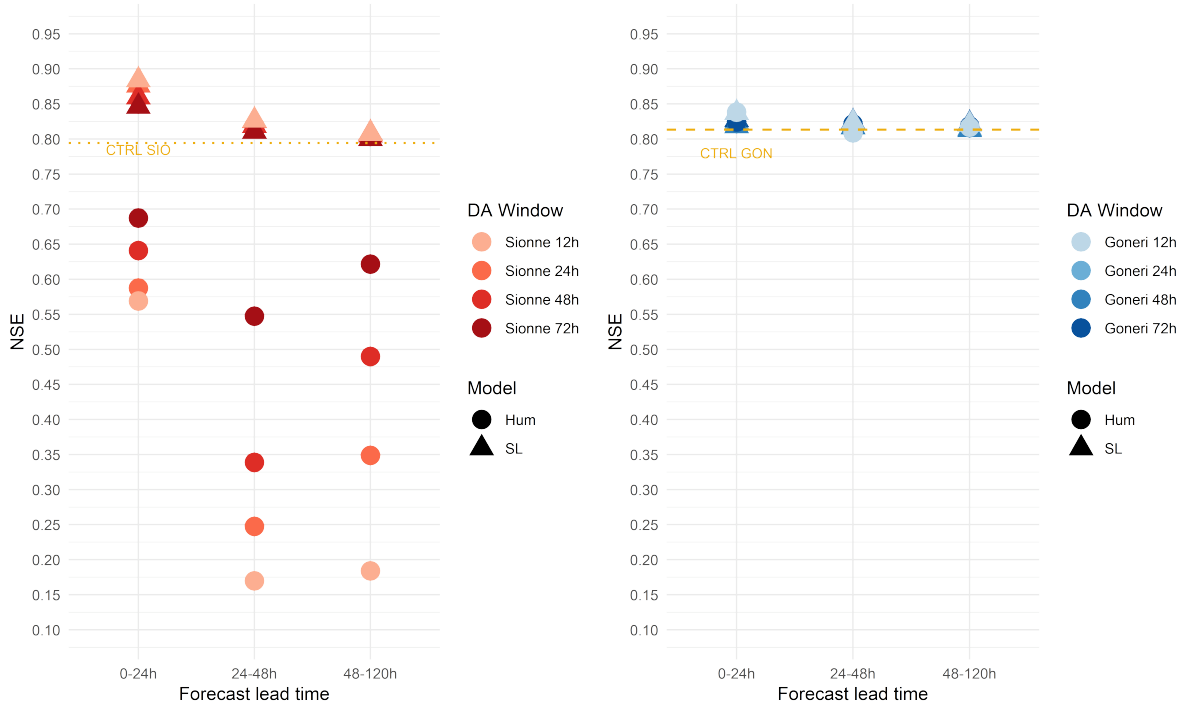

Figure 18 – Method RVB: Results of the global indicator (NSE) for the different DA window during the forecast

Table 8 – Numerical results of NSE indicators along forecast horizon for each of the implemented scenarios according to each catchment using method RVB.

Method RVB									
SIO		12h		24h		48h		72h	
		Hum	SL	Hum	SL	Hum	SL	Hum	SL
	CTRL				0.79				
	0-24h	0.569	0.884	0.587	0.876	0.641	0.860	0.687	0.846
	24-48h	0.170	0.827	0.248	0.826	0.339	0.819	0.547	0.811
	48-120h	0.184	0.808	0.349	0.808	0.490	0.805	0.622	0.800
GON		12h		24h		48h		72h	
		Hum	SL	Hum	SL	Hum	SL	Hum	SL
	CTRL				0.81				
	0-24h	0.838	0.837	0.833	0.824	0.822	0.818	0.825	0.827
	24-48h	0.809	0.823	0.812	0.817	0.815	0.817	0.822	0.824
	48-120h	0.817	0.821	0.817	0.815	0.816	0.813	0.819	0.822

5.3.2 Discussion

Different data assimilation responses

Similar behavior emerges for both watersheds with the OF method, but a difference is noticeable depending on the type of variable updated. This method could be influenced by the linearity of the updated system. In fact, the change in the Hum variable results in a cascading response through the compartments of the HBVS model and consequently leads to a non-linear response of the system. A larger sample size needs to be introduced in the data assimilation to compensate for this effect. This could explain the fact that an improvement of the global performance is observed with a longer assimilation length. However, the effect on the forecasts remains constant and rather poor. Contrary to the SL variant, the update of its conditions will have a direct and linear impact on the flow. This scenario shows promising results in NSE score for the assimilation and for the hydrological forecasts during the 12h assimilation with a maximum enhancement of 12% and 8% for the Sionne and Goneri, respectively, compared to the control simulation.

With the use of the RVB method, two opposite responses stand out for each of the watersheds. An improvement during the assimilation with the Hum variant for the Goneri, while the results are better with the SL variant for the Sionne. This tendency would be explained by the fact that each of the watersheds does not have the same flow contribution between the base flow and the runoff flow (see Figures 9 and 14). The increase of the contribution of the base flow for the Sionne with the HBVS model allows compensating the difference of simulated and observed flows. The Goneri is characterized by a significant contribution of the runoff flow. Thus, a decrease of the variable Hum permits to slightly decrease the flows; by constraining the variable to its maximum, it generates an increase of the quantity of water entering the upper reservoir SU, which increases the runoff flow. The variant with a 12-hour assimilation window obtains the best short-term scores, but its effect quickly fades after 24 hours of forecasting as it converges to the control simulation. The variable is constrained by the parameter FC providing little variance range. The update of the initial conditions cannot result in a Hum value higher than the FC parameter, the maximal soil moisture storage. The SL variant with 72h assimilation provides the most robust long-term version for the Goneri. The forecasts are most improved in the short term by at most 12% for the Sionne and by at most 3.5% for the Goneri compared to the control version using the RVB method with a 12-hour assimilation window length and the SL variant.

On the one hand, the OF method both gives a better overall performance gain during the assimilation with the SL variant, and it provides better short-term forecasts. The gain generated by the RVB method for the Goneri is inferior and is not propagated in the forecasts. This difference may be related to a lower convergence threshold for the OF method allowing a higher number of iterations. Therefore, considering only the global performance assessment, the most convenient method seems to be the OF method with the SL variant for an assimilation time of 12 hours.

SOCONT and HBVS models

Comparing the assimilation results between the SOCONT and HBVS models, the SOCONT model

shows a better improvement during the assimilation period: 90% for the Sionne and 14% for the Goneri. Such improvement is mainly due to a worst baseline, and, in the end, the performance is still better with HBVS. This difference is consistent with the hypothesis that the performance of the assimilation according to the type of updated variable depends on the initial contribution of flows, either runoff or base flow. Furthermore, the effect on forecasting is not considered in this study for the SOCONT method. A. Foehn et al., 2018 has underlined that hydrological forecasts are highly dependent on the calibrated parameters. Thus, the SOCONT method would not be suitable for reliable decision-making in case of high peak events.

Table 9 – Comparison of the improvement during data assimilation between the initial SOCONT model and the new HBVS model through the NSE score.

	Sionne		**Goneri**	
	SOCONT	HBVS 12h SL RVB	SOCONT	HBVS 12h SL OF
CTRL	0.49	0.79	0.73	0.81
UPDT	0.94	0.96	0.85	0.92
Improvement (%)	90	22	14	11

5.4 Event Scale Performance Assessment

5.4.1 Results

Impact of variable type updated and assimilation window length

Figure 19 and 20 highlight the different events for each of the watersheds according to the type of variable updated. The upper figure provides the result of the past flows after the data assimilation with the OF method, and the lower figure shows the evolution of the initial conditions for each 2h time-step during the event.

For the Sionne event, there is a more pronounced variability between the different assimilation lengths in the Hum variant. A longer assimilation length tends towards the CTRL simulation for each case. It is possible to observe how the system reacts to the change in initial conditions; a faster change occurs with shorter assimilation lengths and a more linear initial condition update with longer assimilation lengths. In the case of the Sionne, the simulated flows are closer to the second observation peak in the Hum variant, whereas the flows in the SL variant do not reach it.

The event in the Goneri basin is illustrated in Figure 20. The graphs reveal that neither the SL variant nor the Hum variant can reproduce this extreme event. The Hum variant tends to decrease the rising flows by decreasing the conditions of the Hum variable before the event. However, it does not manage to correctly reproduce the event as a whole since the humidity compartment quickly becomes completely saturated. Regarding the SL variant, it tries to compensate for the missing flow volume by strongly increasing the initial SL variable, this, without success. It is observed that a 72-hour assimilation length is subject to a more uniform increase in the updated variable compared to other assimilation times that reproduce a peak of initial conditions. The change in these conditions

is most pronounced during a 12 hours assimilation, and one can notice that the downward trend of the peak is slightly better reproduced.

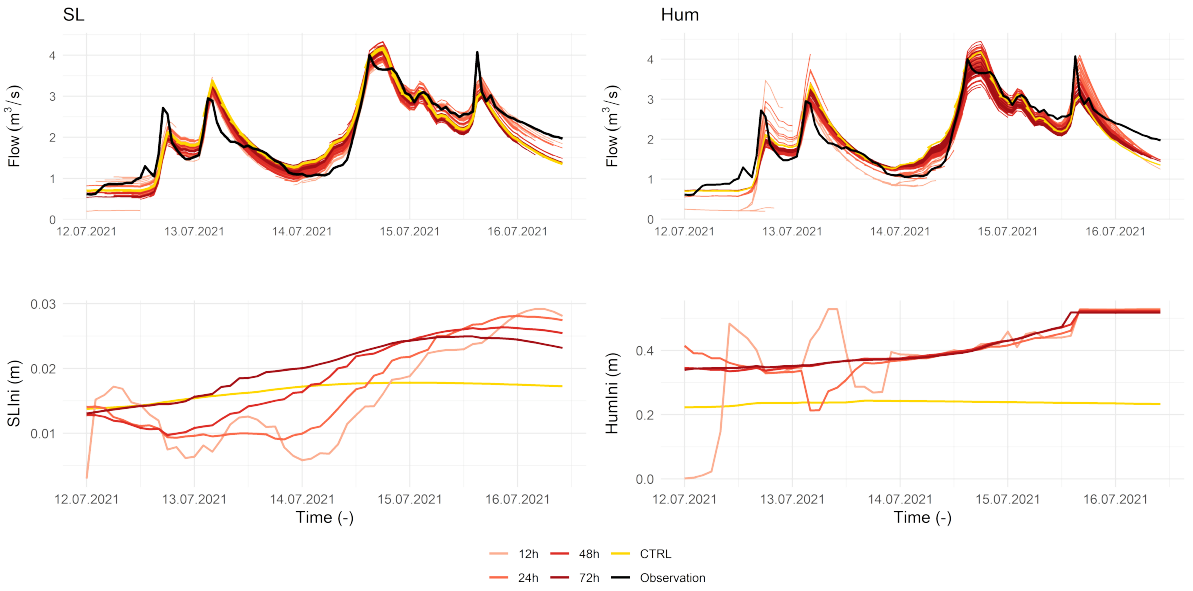

Figure 19 – Illustration of flows obtained after data assimilation and results of changes in initial conditions for each of the updated variables for the Sionne watershed during the July 2021 event.

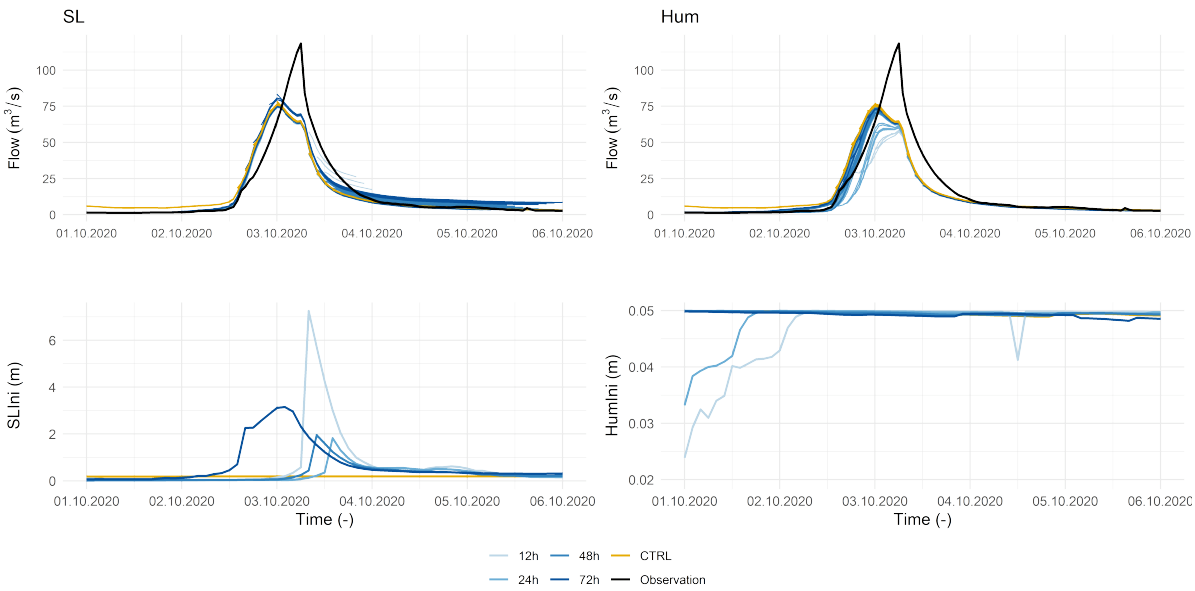

Figure 20 – Illustration of flows obtained after data assimilation and results of changes in initial conditions for each of the updated variables for the Goneri watershed during the October 2020 event.

A second event is presented for Goneri, and this one took place in July 2021. It allows observing a different behavior where the simulated flows are more important than the observed ones. Figure 21 shows that even if the algorithm decreases the SL value to zero, the flows are still exceeded. On the

other hand, updating the Hum variable has a cascading effect on the next reservoir by decreasing the amount of flow coming out of the SU reservoir; therefore, a decrease in flow is observed. The oscillations achievable with a 12h assimilation for the Hum variant offers better results.

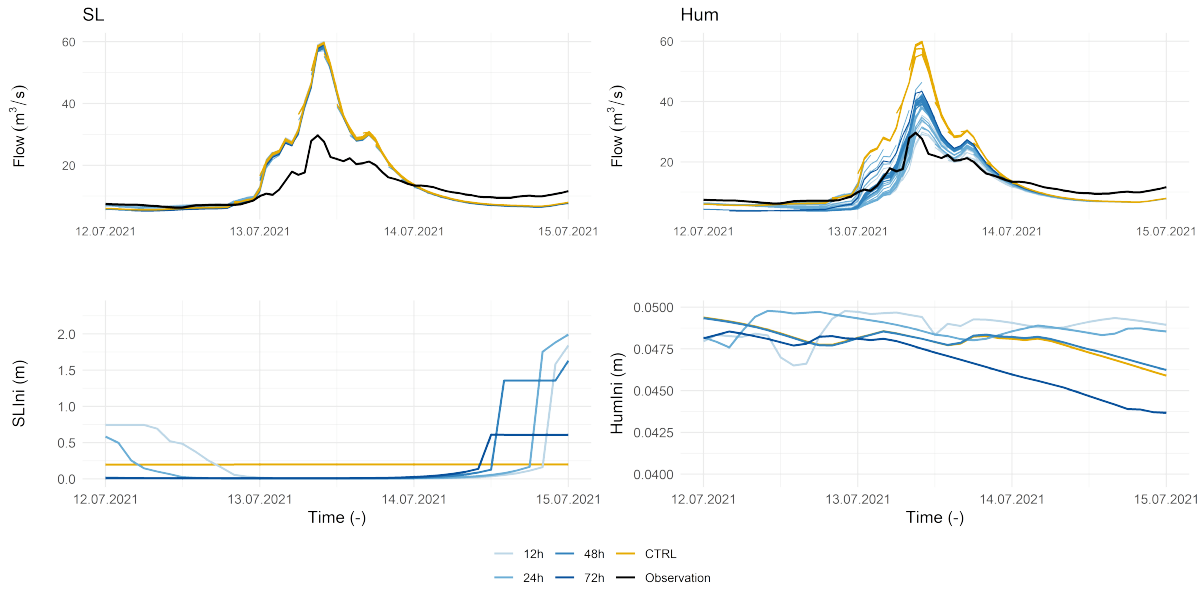

Figure 21 – Illustration of flows obtained after data assimilation and results of changes in initial conditions for each of the updated variables for the Goneri watershed during the July 2021 event.

HBVS and SOCONT comparison

Figure 22 plots the results for the event in July 2021, combining the observations, the SOCONT method, the CTRL version of the HBVS model, and the best assimilation method according to the overall performance, i.e., the OF method with a 12h assimilation on the initial condition of the variable SL. It clearly shows that the HBVS update version converges to the observations, but so does the SOCONT version. Slight differences are noticeable at the two peaks of July 15 and 16. The HBVS model better represents the first peak, while the SOCONT model almost reaches the second peak correctly.

The results for Goneri for the July 2021 period are presented in Figure 23. They include the observations validated by the FOEN, the observations before validation, the OF method for an assimilation time for the SL variant, the HBVS control version and finally, the initial assimilation method SOCONT. First, the updated HBVS version overestimates the peak flows, but the lower flows are well fitted to the observations. Even if the SL variant does not decrease the peak flows, it also shows that on the flows between July 15 and 16, the assimilation allows raising the curve compared to the control version. Concerning the SOCONT version, it should be noted that the assimilated flows correspond to the flows not validated by the FOEN, so the SOCONT curve should tend towards the grey line. However, neither the flood peaks nor the lower flows are reached.

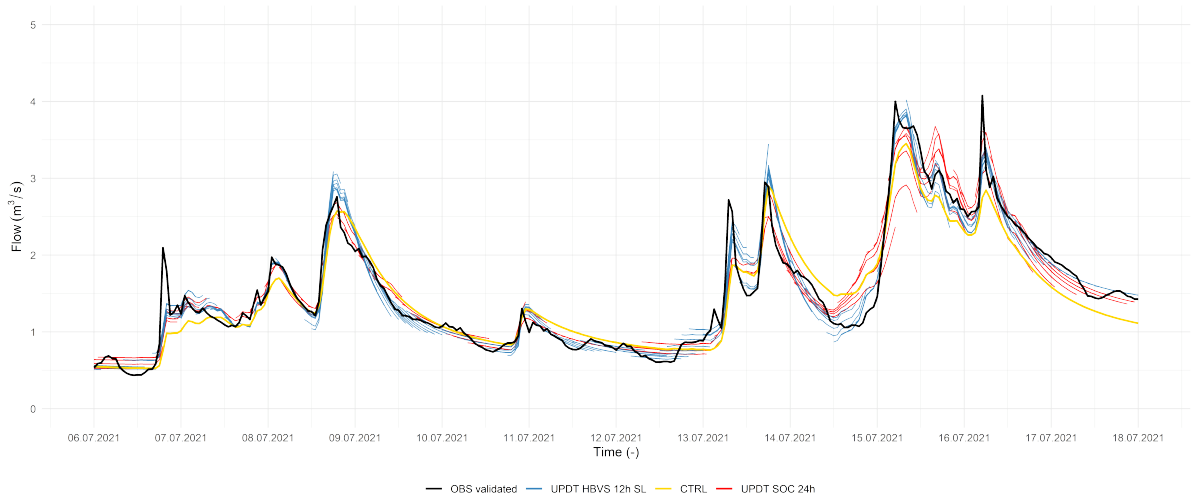

Figure 22 – Comparison of the SL variant for a 12-hour assimilation using the OF method with the results of the SOCONT model assimilation for the Sionne watershed during the event of July 2021.

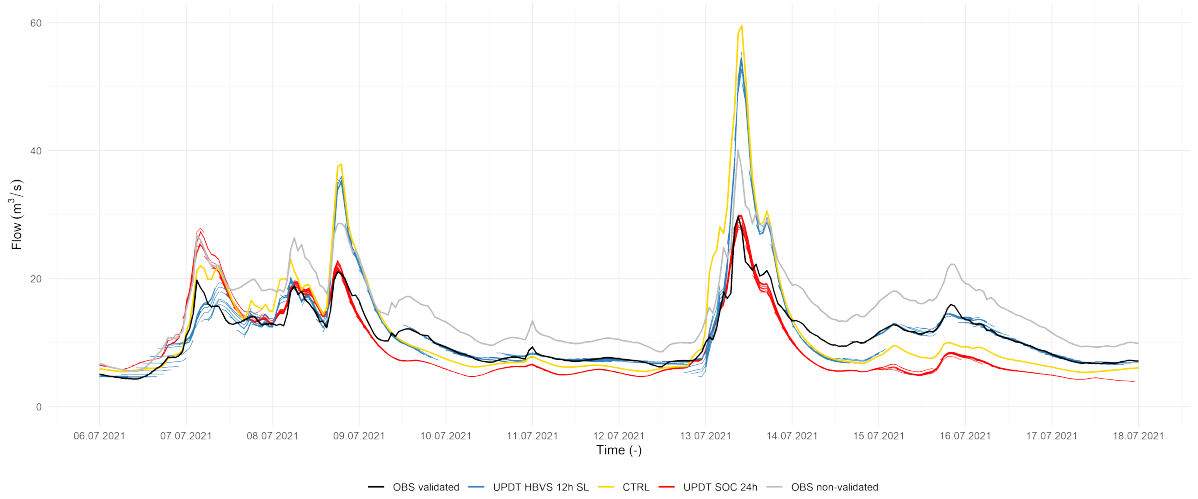

Figure 23 – Comparison of the SL variant for a 12-hour assimilation using the OF method with the results of the SOCONT model assimilation for the GONERI watershed during the event of July 2021. The FOEN non-validated flow observation data are also represented in grey in the graph.

In summary, without considering the impact on hydrological forecasts, the updated version between SOCONT and HBVS is very similar for the Sionne watershed. This is not the case for the Goneri, with a better representation of the flows with the HBVS method.

Variability of forecasts at event scale

Figures 24 and 25 illustrate all the results predicted with the OF method with variant SL for each

basin. They are presented with a 2 hours time step such as the operating system does. For the Sionne watershed, it is noted that the forecasts are more variable for a shorter assimilation period and that they better represent the fluctuations during the event considered. The forecast fluctuations are even greater with the use of the variable Hum, however, they tend towards a too consequent flow overestimation (AppendixC.2).

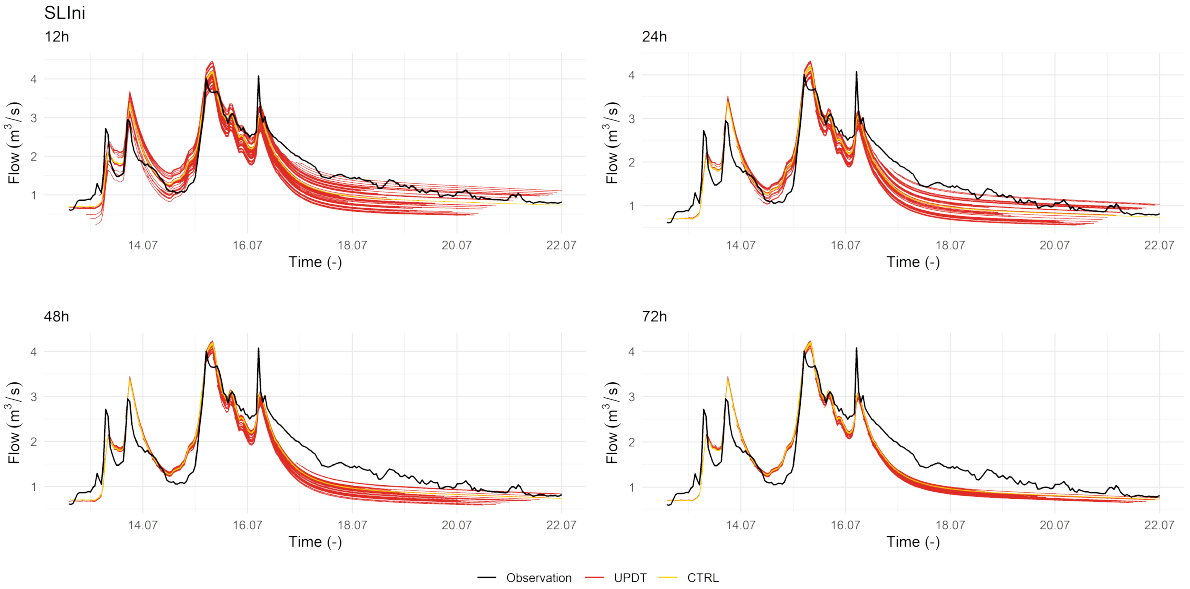

Figure 24 – Variability of hydrological forecasts according to the assimilation window length when updating the SL variable for the Sionne watershed, example of the July 2021 event.

The event of October 2020 does not allow to clearly observe the variations of the forecasts because of the extent of the event, then the event of July 2021 is presented. For Goneri, the fluctuations are very similar for each assimilation length with the method OF (Figure 25).

5.4.2 Discussion

When the assimilation time increases, the system becomes more stable and tends towards the simulation control. The RVB indicator is closer to the null value during the first iteration for a longer assimilation time. Hence, the shorter the assimilation time, the more the number of iterations will potentially increase and thus generate a higher computation cost.

Comparing the type of updated variable on event scale, the Hum initial conditions update has more influence on the Pearson coefficient than the SL variant. This implies that an improvement in the Pearson indicator does not necessarily lead to better results in the simulation and forecast. The relationship between the RVB indicator and the initial conditions Hum seems to be more complex than a simple optimization of the volume in the reservoir. However, it does affect the amount of water leaving the SU reservoir and has an influence on the runoff rate. The variability of forecast

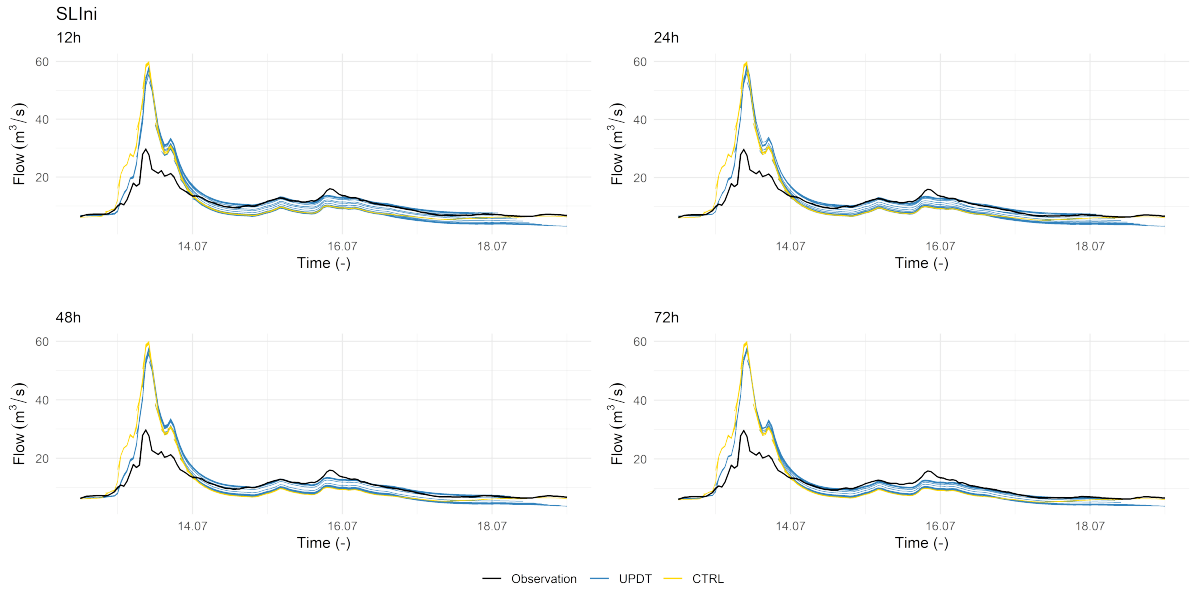

Figure 25 – Variability of hydrological forecasts according to the assimilation window length when updating the SL variable for the Goneri watershed, example of the July 2021 event.

flows makes its use hazardous because it tends to overestimate flows, especially since actual weather forecasts in the real-time operating system also include uncertainties.

The update of the SL initial conditions allows to influence the base flows, which is beneficial for the Sionne because a strong influence exists between the quantity of water in the system and the SL variable: for a change of only 10% in the initial SL conditions, the improvement of RVB indicator is more than 40%. While for the Goneri, the update of the SL variable generates very little change, with less than a 1% improvement of the RVB for a 50% change of the SL variable. The difference in behavior between the RVB and OF method for the SL variable can be explained as follow. The threshold of convergence is immediately exceeded when using the SL variable. By using the Pearson coefficient, which reduces the weighting of the RVB indicator and by having reduced the convergence threshold in the method, an improvement is still possible. However, this improvement has an impact only on low and medium flows and not on peak flows. For the Goneri flood in October 2020, validated observations are most likely subject to errors. Therefore, the judgment of the performance of the model is difficult to correctly assess. SL seems to be unable to reduce the flood peak in case of overestimation, which is a limiting factor of this technique because it will generate false alarms in the operational system.

Assuming that the system is able to adapt appropriately, an improvement of the influence of the SL variable could be achieved by adjusting the related parameters, i.e., by manually increasing the base flow storage coefficient k_L, for instance. Further investigations will have to be achieved to determine precisely how much the parameter should be increased.

5.5 Outlook : Long Term Assimilation Period for Model Error Identification

The data assimilation technique used does not allow to quantify the uncertainties on the model results, however the results obtained from the update of the initial conditions might be helpful to identify the error trends of the model, for instance, by analyzing the new SL initial conditions updated during the data assimilation compared to the control version ones (Figure 26).

We observe that, for the Sionne, the HBVS model overestimates the flows between February and early June, a phenomenon potentially related to the withdrawal of the bisses or to the overestimation of precipitation. Contrary to Goneri, the model tends to underestimate flows during the snowmelt period between March and May. This type of evaluation would provide an estimate of the volumes of water artificially introduced into the system and would offer a basis for directing improvements in the model parameters.

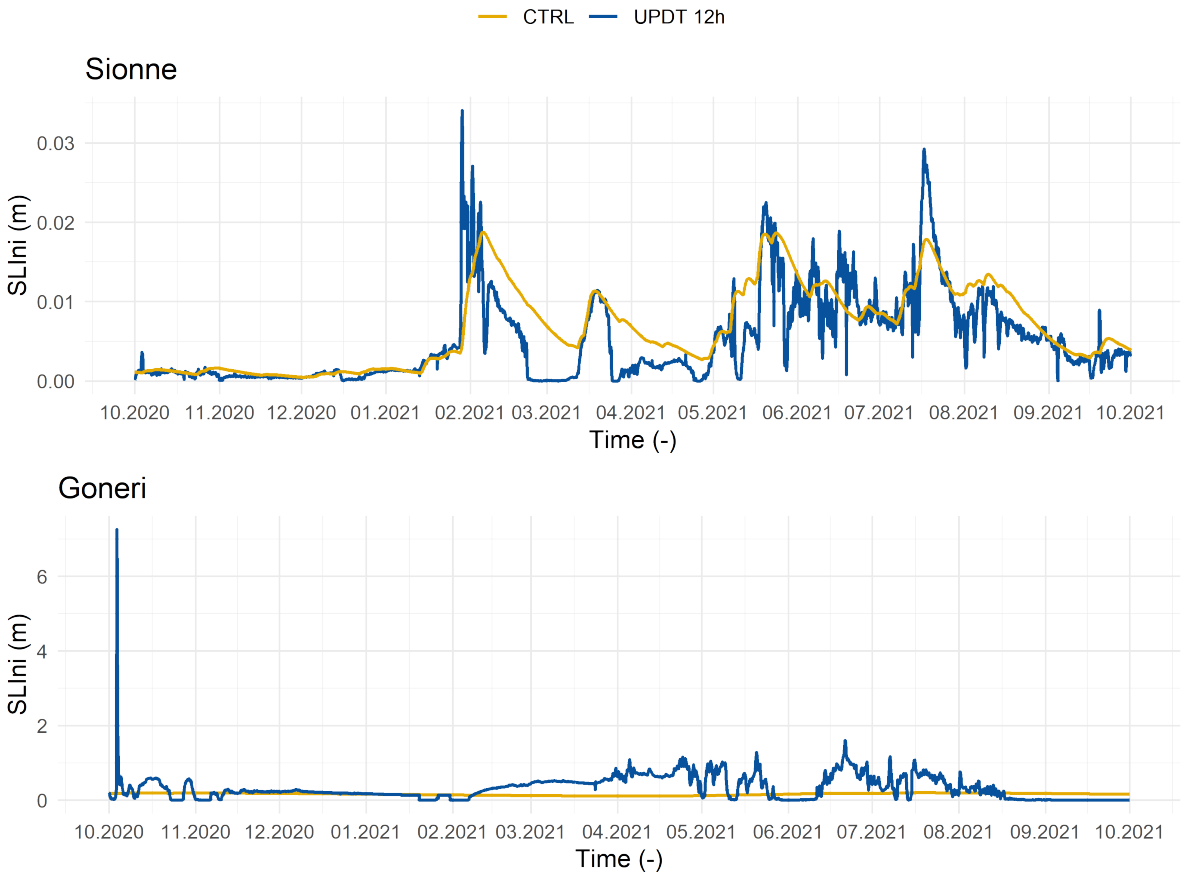

Figure 26 – Overview of the change in SL initial conditions during data assimilation with a 12-hour assimilation window length over the period from October 1, 2020 to October 1, 2021.

6 Conclusion

The recent calibration of the HBVS model for the Sionne and Morge watersheds has shown that the initial SOCONT models do not correctly represent seasonal dynamics and base flows. Higher compartmentalization of the storage reservoirs and the manual calibration of the AlphaU parameter obtain better performance evaluated with the NSE indicator. In general, the HBVS model has the ability to compensate for some uncertainties in the spatial distribution of precipitation or non-modeled withdrawals. This capability ensures that the model is efficient and reliable, which is essential for robust hydrological forecasts. This model also allows a better modelling of the flood peaks. A perspective of improvement would be the use of the KGE (Kling-Gupta efficiency) indicator in the choice of performance metric, which has shown an improvement of flood peak calibrations for a HBV model type (Mizukami et al., 2019).

16 data assimilation implementation schemes have been tested for each of the Sionne and Goneri watersheds. Scenario variations include different assimilation window lengths (12h, 24h, 48h and 72h) a different type of updated variable (the soil moisture component Hum or the lower reservoir height SL). The evaluation of these implementation schemes is performed with one year of simulation of the operating system using weather observations as forecasts and qualitative analysis of the significant events during this period. trends can be distinguished in the scenario analysis according to the variable type: shorter assimilation has a more beneficial gain on the SL variant, unlike the Hum variable. A larger assimilation window length tends to decrease the variability of the forecasts and converge to the control simulation, while a small assimilation window length shows more variability between time-step.

The variant with the update of the variable Hum tends to a solution that converges in a non-optimal direction in terms of update simulation and hydrological forecasts, on the one hand by results of global performance little encouraging and on the other hand by a substantial variability of the forecasts, which is susceptible to bias the assessments for support to decision making. Relation between soil humidity and discharges reveals to be more complex via a cascading effect through the model compartments, and methods analyzed in this study are unable to solve such optimization due to non-linearity in response.

The SL variant with an assimilation window length shows the best overall performance compared to the control simulation with a beneficial gain on short-term forecasts, between 0-24h lead time. However, the contribution between runoff and base flows is distinct for an alpine nival regime such as Sionne or a nivo-glacial regime such as Goneri and is observed by a difference of the parameters related to the SL reservoirs. A weak contribution of the SL reservoir as for the Goneri watershed implies that its update has little influence on the RVB indicator and leads to a rapid reaching of the convergence threshold. By decreasing the weighting of this indicator using the OF method, better performances are then obtained. A computation cost is more important for such a method; using the RVB method with a lower convergence threshold would be possible. Following the evaluation of the assimilation lengths, shorter assimilation, i.e., 12h instead of 24h initially, leads to an increase in the number of iterations and a more consequent margin of improvement.

However, the SL variable seems to have little influence on the flood peaks, which remain difficult to reach. It suggests that the model parameters, in other words, the calibration, probably play a role in the performance of the data assimilation. Even if the amplitude of the flood peak is still uncertain, an event like the Goneri flood in October is very beneficial for the reliability of the model parameters during a significant event, contrary to the Sionne, where no major event is observed. A rapid response that has not been calibrated beforehand is challenging to reproduce.

It is possible that by allowing a more considerable margin of freedom to the SL reservoir parameters and considering that the model can compensate for these effects through data assimilation, better reproduction of flood peaks could occur. Further inversions must be undertaken on the extent of possible modifications. A set of iterations on the whole set of variables could also offer good results but would generate a higher computational cost for implementation in the operational system.

This thesis shows that significant improvements are possible with the new HBVS model for the studied watersheds. Data assimilation reduces the errors in hydrological modeling, implying that the propagation of errors in hydrological forecasts in the real-time operating system would then be more related to the uncertainties of weather forecast. Nonetheless, the solution proposed in this study may allow an overall better performance of operational forecasts and could hence have a positive impact on flood monitoring and mitigation in Valais.

References

Abbaszadeh, P., Moradkhani, H., & Daescu, D. N. (2019). The Quest for Model Uncertainty Quantification: A Hybrid Ensemble and Variational Data Assimilation Framework. *Water Resources Research*, *55*(3), 2407–2431. https://doi.org/10.1029/2018WR023629

Abbaszadeh, P., Moradkhani, H., & Yan, H. (2018). Enhancing hydrologic data assimilation by evolutionary Particle Filter and Markov Chain Monte Carlo. *Advances in Water Resources*, *111*, 192–204. https://doi.org/10.1016/j.advwatres.2017.11.011

Ancey, C. (2020). Risques hydrologiques aménagemenett du territoire, 340.

Baracchini, T. (2021). *Calibration RS MINERVE des bassins versants du Haut-Valais, Projet MINERVE - Développement 2021* (tech. rep.). Sion.

Bergström, S. (1976). Development and application of a conceptual runoff model for scandinavian catchments.

Da Ros, D., & Borga, M. (1997). Adaptive Use of a Conceptual Model for Real Time Flood Forecasting. *Hydrology Research*, *28*(3), 169–188. https://doi.org/10.2166/nh.1997.0010

Duan, Q. Y., Gupta, V. K., & Sorooshian, S. (1993). Shuffled complex evolution approach for effective and efficient global minimization. *Journal of Optimization Theory and Applications*, *76*(3), 501–521. https://doi.org/10.1007/BF00939380

Dumedah, G., & Coulibaly, P. (2013). Evolutionary assimilation of streamflow in distributed hydrologic modeling using in-situ soil moisture data. *Advances in Water Resources*, *53*, 231–241. https://doi.org/10.1016/j.advwatres.2012.07.012

Evensen, G. (1994). Sequential data assimilation with a nonlinear quasi-geostrophic model using Monte Carlo methods to forecast error statistics. *Journal of Geophysical Research: Oceans*, *99*(C5), 10143–10162. https://doi.org/10.1029/94JC00572

Fan, Y., Huang, G., Baetz, B., Li, Y., Huang, K., Chen, X., & Gao, M. (2017). Development of integrated approaches for hydrological data assimilation through combination of ensemble Kalman filter and particle filter methods. *Journal of Hydrology*, *550*, 412–426. https://doi.org/10.1016/j.jhydrol.2017.05.010

Foehn, A., García Hernández, J., Schaefli, B., & De Cesare, G. (2018). Spatial interpolation of precipitation from multiple rain gauge networks and weather radar data for operational applications in Alpine catchments. *Journal of Hydrology*, *563*, 1092–1110. https://doi.org/10.1016/j.jhydrol.2018.05.027

Foehn, A. T. (2019). Radar-rain gauge merging and discharge data assimilation for flood forecasting in alpine catchments.

FOEN, O. f. d. l. (2020a). Changements climatiques en Suisse. Retrieved March 13, 2022, from https://www.bafu.admin.ch/bafu/fr/home/themen/thema-klima/klima--publikationen-und-studien/publikationen-klima/klimaaenderung-in-der-schweiz.html

FOEN, O. f. d. l. (2020b). Magazine «l'environnement» 2/2020 – Tous concernés ! Retrieved March 13, 2022, from https://www.bafu.admin.ch/bafu/fr/home/themen/thema-naturgefahren/naturgefahren--publikationen/publikationen-naturgefahren/magazin-umwelt-2-2020-naturgefahren-gehen-alle-an.html

Garcia Hernández, J., Foehn, A., Fluixá-Sanmartín, J., Roquier, B., Paredes Arquiola, P., De Cesare, G., & Brauchli, T. (2020). *RSMINERVE – Technical manual, v2.25* (tech. rep.). Ed. CREALP. Switzerland.

Gremaud, V., Goldscheider, N., Savoy, L., Favre, G., & Masson, H. (2009). Geological structure, recharge processes and underground drainage of a glacierised karst aquifer system, Tsanfleuron-Sanetsch, Swiss Alps. *Hydrogeology Journal*, *17*(8), 1833–1848. https://doi.org/10.1007/s10040-009-0485-4

Hernández, F., & Liang, X. (2017). *Hybridizing Bayesian and variational data assimilation for robusthigh-resolution hydrologic forecasting* (preprint). Hillslope hydrology/Modelling approaches. https://doi.org/10.5194/hess-2017-431

Hernández, J. G., Boillat, J.-L., Jordan, F., & Hingray, B. (2009). La prévision hydrométéorologique sur le bassin versant du Rhône en amont du Léman [Number: 5 Publisher: EDP Sciences]. *La Houille Blanche*, (5), 61–70. https://doi.org/10.1051/lhb/2009057

Javaheri, A., Nabatian, M., Omranian, E., Babbar-Sebens, M., & Noh, S. (2018). Merging Real-Time Channel Sensor Networks with Continental-Scale Hydrologic Models: A Data Assimilation Approach for Improving Accuracy in Flood Depth Predictions. *Hydrology*, *5*(1), 9. https://doi.org/10.3390/hydrology5010009

Jordan, F. (2007). Modèle de prévision et de gestion des crues:optimisation des opérations des aménagements hydroélectriques à accumulation pour la réduction des débits de crue.

Lee, H., Seo, D.-J., & Koren, V. (2011). Assimilation of streamflow and in situ soil moisture data into operational distributed hydrologic models: Effects of uncertainties in the data and initial model soil moisture states. *Advances in Water Resources*, *34*(12), 1597–1615. https://doi.org/10.1016/j.advwatres.2011.08.012

Lei, L., & Hacker, J. P. (2015). Nudging, Ensemble, and Nudging Ensembles for Data Assimilation in the Presence of Model Error [Publisher: American Meteorological Society Section: Monthly Weather Review]. *Monthly Weather Review*, *143*(7), 2600–2610. https://doi.org/10.1175/MWR-D-14-00295.1

Lindström, G., Johansson, B., Persson, M., Gardelin, M., & Bergström, S. (1997). Development and test of the distributed HBV-96 hydrological model. *Journal of Hydrology*, *201*(1-4), 272–288. https://doi.org/10.1016/S0022-1694(97)00041-3

Liu, S., Shao, Y., Yang, C., Lin, Z., & Li, M. (2012). Improved regional hydrologic modelling by assimilation of streamflow data into a regional hydrologic model. *Environmental Modelling & Software*, *31*, 141–149. https://doi.org/10.1016/j.envsoft.2011.12.005

Liu, Y., Weerts, A. H., Clark, M., Hendricks Franssen, H.-J., Kumar, S., Moradkhani, H., Seo, D.-J., Schwanenberg, D., Smith, P., van Dijk, A. I. J. M., van Velzen, N., He, M., Lee, H., Noh, S. J., Rakovec, O., & Restrepo, P. (2012). Advancing data assimilation in operational hydrologic forecasting: progresses, challenges, and emerging opportunities. *Hydrology and Earth System Sciences*, *16*(10), 3863–3887. https://doi.org/10.5194/hess-16-3863-2012

Meteoswiss. (2021). https://www.meteoswiss.admin.ch

Mizukami, N., Rakovec, O., Newman, A. J., Clark, M. P., Wood, A. W., Gupta, H. V., & Kumar, R. (2019). On the choice of calibration metrics for “high-flow” estimation using hydrologic models

[Publisher: Copernicus GmbH]. *Hydrology and Earth System Sciences*, *23*(6), 2601–2614. https://doi.org/10.5194/hess-23-2601-2019

National Centre for Climate Services. (2018). *CH2018 – Climate Scenarios for Switzerland, Technical Report* (tech. rep.). Zurich.

Park, S. K., & Xu, L. (Eds.). (2017). *Data Assimilation for Atmospheric, Oceanic and Hydrologic Applications (Vol. III)*. Springer International Publishing. https://doi.org/10.1007/978-3-319-43415-5

Pathiraja, S., Marshall, L., Sharma, A., & Moradkhani, H. (2016). Hydrologic modeling in dynamic catchments: A data assimilation approach. *Water Resources Research*, *52*(5), 3350–3372. https://doi.org/10.1002/2015WR017192

Quefféléan, C., Y. (2015). Evaluation du temps de montée des crues torrentielles rapides, 200.

R Core Team. (2019). *R: a language and environment for statistical computing*. R Foundation for Statistical Computing. Vienna, Austria. https://www.R-project.org/

Rafieeinasab, A., Seo, D.-J., Lee, H., & Kim, S. (2014). Comparative evaluation of maximum likelihood ensemble filter and ensemble Kalman filter for real-time assimilation of streamflow data into operational hydrologic models. *Journal of Hydrology*, *519*, 2663–2675. https://doi.org/10.1016/j.jhydrol.2014.06.052

Reichle, R. H., McLaughlin, D. B., & Entekhabi, D. (2002). Hydrologic Data Assimilation with the Ensemble Kalman Filter. *Monthly Weather Review*, *130*(1), 103–114. https://doi.org/10.1175/1520-0493(2002)130<0103:HDAWTE>2.0.CO;2

Reynard, E. (2002). Hill irrigation in Valais (Swiss Alps). Recent evolution of common-property corporations., 11.

Samuel, J., Rousseau, A. N., Abbasnezhadi, K., & Savary, S. (2019). Development and evaluation of a hydrologic data-assimilation scheme for short-range flow and inflow forecasts in a data-sparse high-latitude region using a distributed model and ensemble Kalman filtering. *Advances in Water Resources*, *130*, 198–220. https://doi.org/10.1016/j.advwatres.2019.06.004

Seo, D.-J., Koren, V., & Cajina, N. (2003). Real-Time Variational Assimilation of Hydrologic and Hydrometeorological Data into Operational Hydrologic Forecasting. *Journal of Hydrometeorology*, *4*(3), 627–641. https://doi.org/10.1175/1525-7541(2003)004<0627:RVAOHA>2.0.CO;2

Singh, V. P., & Woolhiser, D. A. (2002). Mathematical Modeling of Watershed Hydrology. *Journal of Hydrologic Engineering*, *7*(4), 270–292. https://doi.org/10.1061/(ASCE)1084-0699(2002)7:4(270)

Vannier, O., Anquetin, S., & Braud, I. (2016). Investigating the role of geology in the hydrological response of Mediterranean catchments prone to flash-floods: Regional modelling study and process understanding. *Journal of Hydrology*, *541*, 158–172. https://doi.org/10.1016/j.jhydrol.2016.04.001

WEF, W. E. F. (2020). *The Global Risks Report 2020, 15th Edition* (tech. rep.). https://www3.weforum.org/docs/WEF_Global_Risk_Report_2020.pdf

Weingartner, R., Barben, M., & Spreafico, M. (2003). Floods in mountain areas—an overview based on examples from Switzerland. *Journal of Hydrology*, *282*(1), 10–24. https://doi.org/10.1016/S0022-1694(03)00249-X

WMO, W. M. O. (2021). Water-related hazards dominate disasters in the past 50 years. Retrieved March 16, 2022, from https://public.wmo.int/en/media/press-release/water-related-hazards-dominate-disasters-past-50-years

A Global context

A.1 Land cover

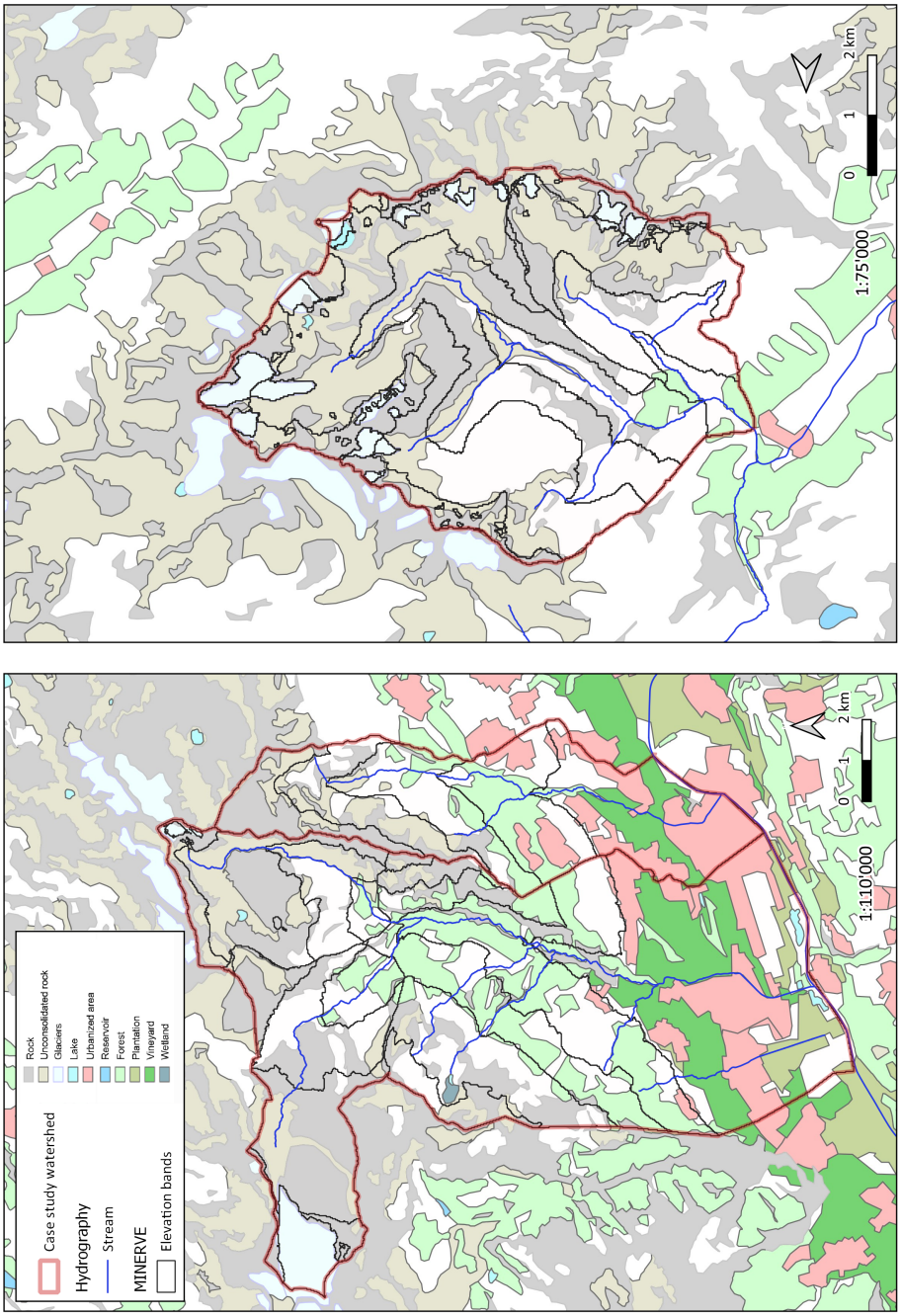

Figure 27 – Land cover for the Sionne, Morge (left) and Goneri (right) watersheds from the swissTLM-Regio Landcover (Federal Office of Topography swisstopo)

A.2 Geological features

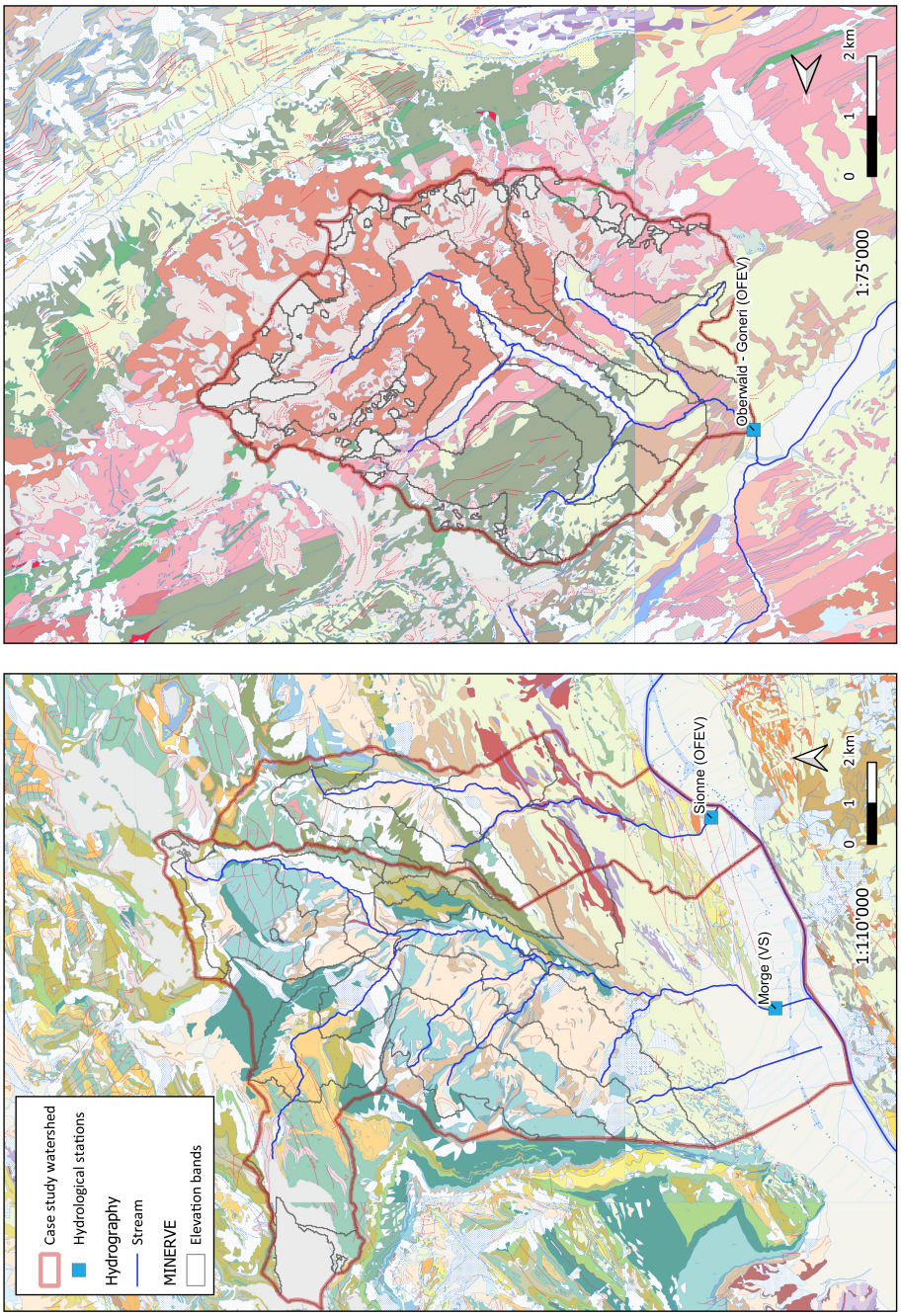

Figure 28 – Geological map for the Sionne, Morge (left) and Goneri (right) watersheds from the Geological Vector Datasets GeoCover (Federal Office of Topography swisstopo).

A.3 Concentration time: detailed calculation

Kirpich formule (1940)[9] :

$$t_c = 19.47 \cdot 10^{-3} \frac{L^{0.77}}{i^{0.385}}$$

with t_c : The concentration time $[min]$
L : The hydraulic pathway $[m]$
i : The average stream slope [%]

Quefféléan formule (Quefféléan, 2015) :

$$t_c = \frac{0.077}{0.375} \cdot S^{0.55}$$

with t_c : The concentration time $[h]$
S : The surface area of the catchment $[km^2]$

[9] Based on Ancey, 2020

A.4 Bisses water intakes

(a) Bitailla

(b) Bisse of Lentine

(c) Bisse of Grimisuat

Figure 29 – Exemples of water intakes from the Sionne (*Source: Musée valaisan des bisses and Camptocamp*)

A.5 Availability and quality of meteorological data

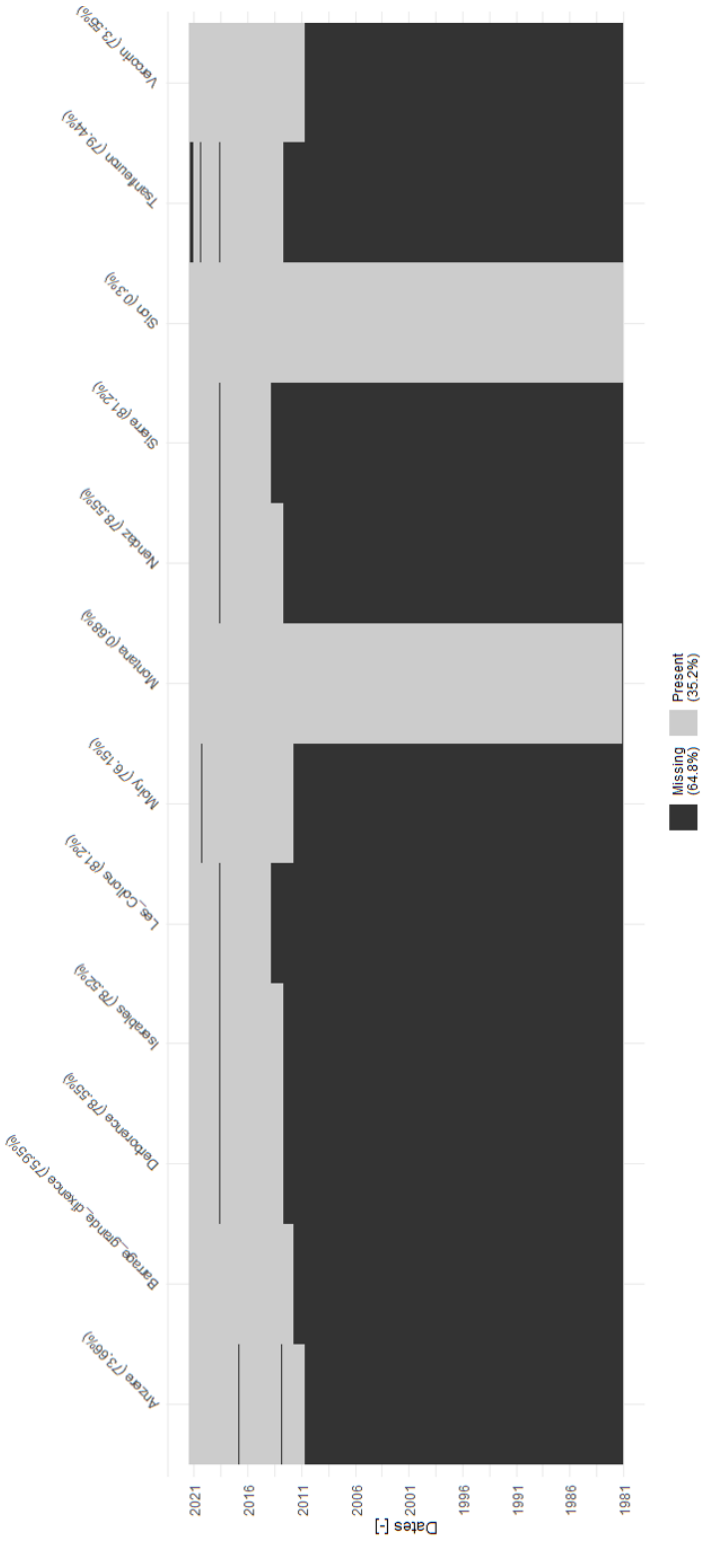

A.6 Studied hydrological period and event for each watershed

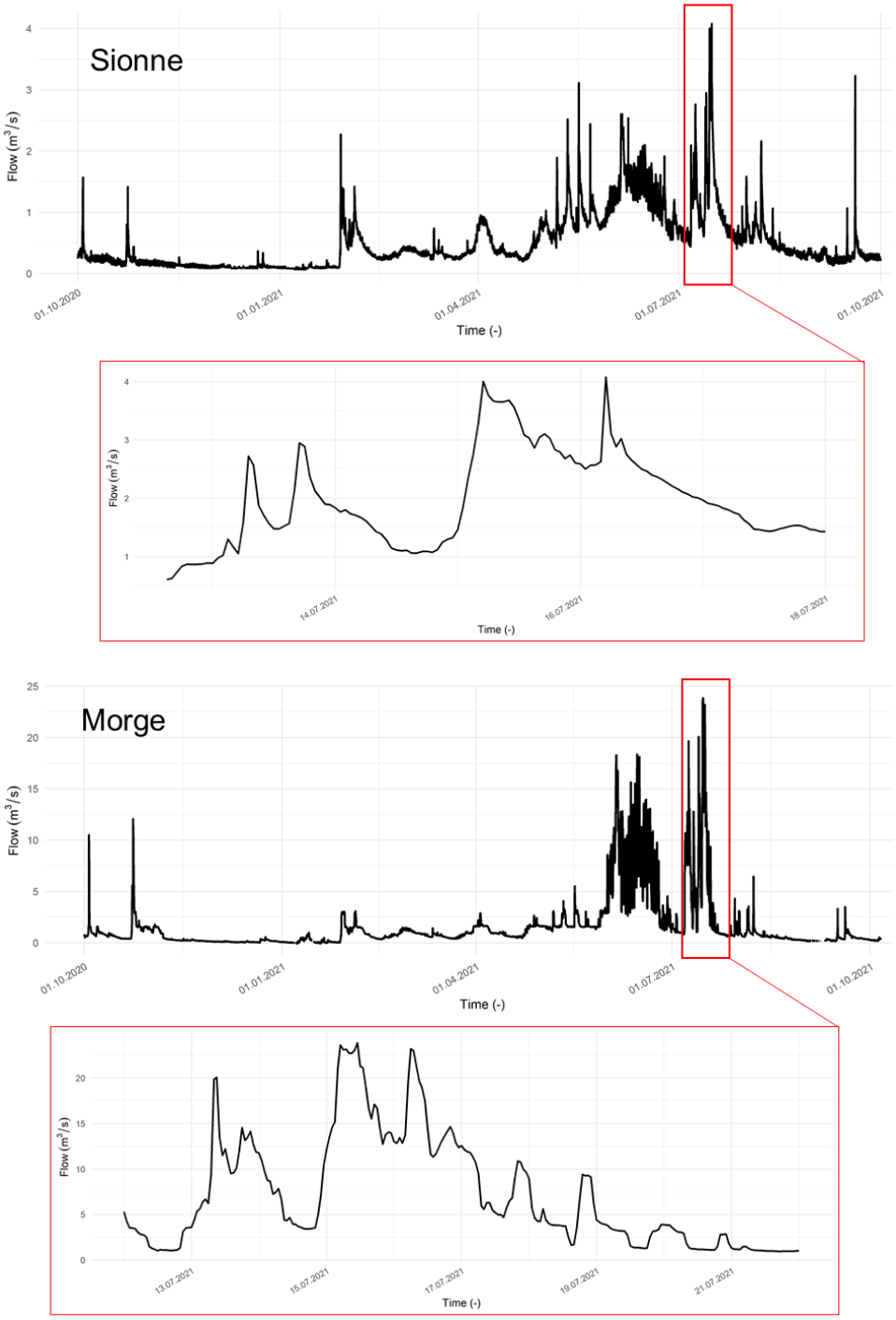

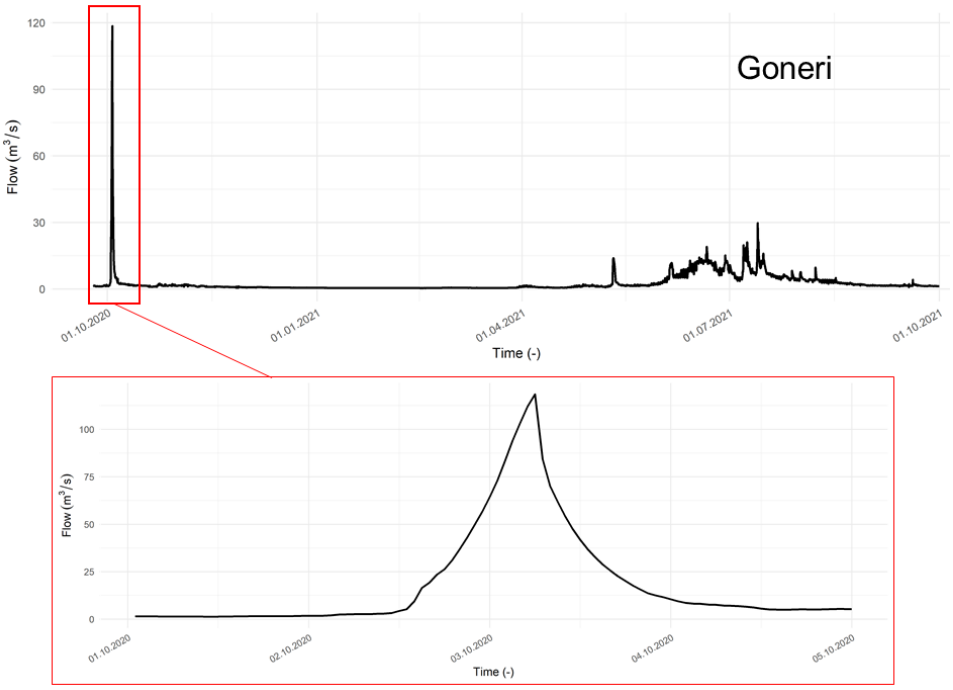
Goneri
120
90
60
30
0
Flow (m3/s)
01.10.2020
01.01.2021
01.04.2021
01.07.2021
01.10.2021
Time (-)
100
75
50
25
0
Flow (m3/s)
01.10.2020
02.10.2020
03.10.2020
04.10.2020
05.10.2020
Time (-)

B Calibration

B.1 Performance indicators

- **Nash-Sutcliffe (Nash)**: varies from $-\infty$ to 1, with 1 representing the best performance.

$$Nash = 1 - \frac{\sum_{t=t_i}^{t^f}(Q_{sim,t} - Q_{obs,t})^2}{\sum_{t=t_i}^{t^f}(Q_{sim,t} - \overline{Q}_{obs})^2} \tag{6}$$

with $Q_{obs,t}$: Observed discharge $[m^3/s]$
$Q_{sim,t}$: Simulated discharge $[m^3/s]$
$\overline{Q}_{obs}$: Average observed discharge $[m^3/s]$

- **Pearson Correlation Coefficient**: varies from -1 to 1, with 1 representing the best performance.

$$Pearson = \frac{\sum_{t=t_i}^{t^f}(Q_{sim,t} - \overline{Q}_{sim}) \cdot (Q_{obs,t} - \overline{Q}_{obs})}{\sqrt{\sum_{t=t_i}^{t^f}(Q_{sim,t} - \overline{Q}_{sim})^2 \cdot \sum_{t=t_i}^{t^f}(Q_{obs,t} - \overline{Q}_{obs})^2}} \tag{7}$$

with $\overline{Q}_{sim}$: Average simulated discharge $[m^3/s]$

- **Relative Volume Biais (RVB)**: varies from -1 to ∞, with 0 representing the best performance.

$$RVB = \frac{\sum_{t=t_i}^{t^f}(Q_{sim,t} - Q_{obs,t})}{\sum_{t=t_i}^{t^f} Q_{obs,t}} \tag{8}$$

- **Root mean square error (RMSE)**: varies from 0 to ∞, with 0 representing the best performance.

$$RMSE = \sqrt{\frac{\sum_{t=t_i}^{t^f}(Q_{sim,t} - Q_{obs,t})^2}{n}} \tag{9}$$

with n: Number of values[−]

B.2 Initial and calibrated parameters

Table 10 – List of calibrated parameters for the HBVS model and initial parameters for the SOCONT model.

SIONNE

SOCONT		**HBVS**	
Gradient T (°C/m)	-0.0054	Gradient T (°C/m)	-0.0048
CFR (-)	1	CFMax (mm/°C/d)	3.6
SInt (mm/°C/d)	0	CFR (-)	0.3
SMin (mm/°C/d)	0	CWH (-)	0.1
SPh (d)	80	TT (°C)	1.0
ThetaCri (-)	0.1	TTInt (°C)	2
bp (d/mm)	0.0125	TTSM (°C)	0
Tcp1 (°C)	0	Beta (-)	1.48
Tcp2 (°C)	4	FC (mm)	490
Tcf (°C)	0	PWP (-)	0.03
HGR3Max (m)	0.8	SUMax (mm)	0
KGR3 (1/s)	0.00025	Ku (1/d)	0.065
Kr (1/s)	0.5	Kl (1/d)	0.059
		Kperc (1/d)	0.559
		SRF (mm/W/d)	4.60E-06
		AlphaU (-)	1.72
		AlphaU (-)	1.72

MORGE

SOCONT		**HBVS**	
Gradient T (°C/m)	-0.0047	Gradient T (°C/m)	-0.0047
CFR (-)	1	CFFmax	2.90
SInt (mm/°C/d)	4.00	CFR (-)	1
SMin (mm/°C/d)	0.87	CWH (-)	0.12
SPh (d)	80	TT (°C)	1.52
ThetaCri (-)	0.1	TTInt (°C)	0
bp (d/mm)	0.0125	TTSM (°C)	0
Tcp1 (°C)	0	Beta (-)	3.19
Tcp2 (°C)	4	FC (mm)	447
Tcf (°C)	0	PWP (-)	0.41
HGR3Max (m)	0.758	SUMax (mm)	0
KGR3 (1/s)	0.00025	Ku (1/d)	0.078
Kr (1/s)	0.10	Kl (1/d)	6.9E-05
		Kperc (1/d)	0.362
		SRF (mm/W/d)	5.6E-05
		AlphaU (-)	1.95

GSM			
S (mm/°C/d)	7.204	S (mm/°C/d)	3.953
CFR (-)	1	CFR (-)	1
SInt (mm/°C/d)	0	SInt (mm/°C/d)	0.011
SMin (mm/°C/d)	0	SMin (mm/°C/d)	0
Sph (d)	80	Sph (d)	80
ThetaCri (-)	0.1	ThetaCri (-)	0.1
bp (d/mm)	0.0125	bp (d/mm)	0.0125
Tcp1 (°C)	0	Tcp1 (°C)	0
Tcp2 (°C)	4	Tcp2 (°C)	4
Tcf (°C)	0	Tcf (°C)	0
SRF (mm/W/d)	0.525	SRF (mm/W/d)	0.669
Ice Albedo (%)	0.35	Ice Albedo (%)	0.35
G (mm/°C/d)	0.010	G (mm/°C/d)	0.017
GInt (mm/°C/d)	0	GInt (mm/°C/d)	0.821
GMin (mm/°C/d)	0	GMin (mm/°C/d)	0.007
Tcg (°C)	0	Tcg (°C)	0.321
Kgl (1/d)	2.5	Kgl (1/d)	1.20
Ksn (1/d)	2.4	Ksn (1/d)	2.00
IRF (mm/W/d)	0.2094	IRF (mm/W/d)	0.523

GONERI			
SOCONT		**HBVS**	
Gradient T (°C/m)	1	Gradient T (°C/m)	-0.0039
CFR (-)	0	CFFmax	1.93
SInt (mm/°C/d)	0	CFR (-)	0.15
SMin (mm/°C/d)	80	CWH (-)	0.1
SPh (d)	0.1	TT (°C)	1.7
ThetaCri (-)	0.0125	TTInt (°C)	0
bp (d/mm)	0	TTSM (°C)	0
Tcp1 (°C)	4	Beta (-)	5.0
Tcp2 (°C)	0	FC (mm)	50.0
Tcf (°C)	0.2	PWP (-)	0.4
HGR3Max (m)	0.0004	SUMax (mm)	0
KGR3 (1/s)	500	Ku (1/d)	0.078
Kr (1/s)	0.3	Kl (1/d)	6.9E-05
		Kperc (1/d)	0.09
		SRF (mm/W/d)	2.7E-05
		AlphaU (-)	2.9
GSM			
S (mm/°C/d)	3	S (mm/°C/d)	5.84
CFR (-)	1	CFR (-)	0.08
SInt (mm/°C/d)	0	SInt (mm/°C/d)	2.75
SMin (mm/°C/d)	0	SMin (mm/°C/d)	0
Sph (d)	80	Sph (d)	326
ThetaCri (-)	0.1	ThetaCri (-)	0.00016
bp (d/mm)	0.0125	bp (d/mm)	0.0125
Tcp1 (°C)	0	Tcp1 (°C)	0
Tcp2 (°C)	4	Tcp2 (°C)	2
Tcf (°C)	0	Tcf (°C)	0
SRF (mm/W/d)	0.0001	SRF (mm/W/d)	0.598
Ice Albedo (%)	0.35	Ice Albedo (%)	0.35
G (mm/°C/d)	15	G (mm/°C/d)	10.3
GInt (mm/°C/d)	0	GInt (mm/°C/d)	3.2
GMin (mm/°C/d)	0	GMin (mm/°C/d)	0
Tcg (°C)	0	Tcg (°C)	0.196
Kgl (1/d)	1.6	Kgl (1/d)	0.188
Ksn (1/d)	1.6	Ksn (1/d)	0.397
IRF (mm/W/d)	0.0001	IRF (mm/W/d)	0.003

C Data assimilation

C.1 Attempt at updating the SU variable

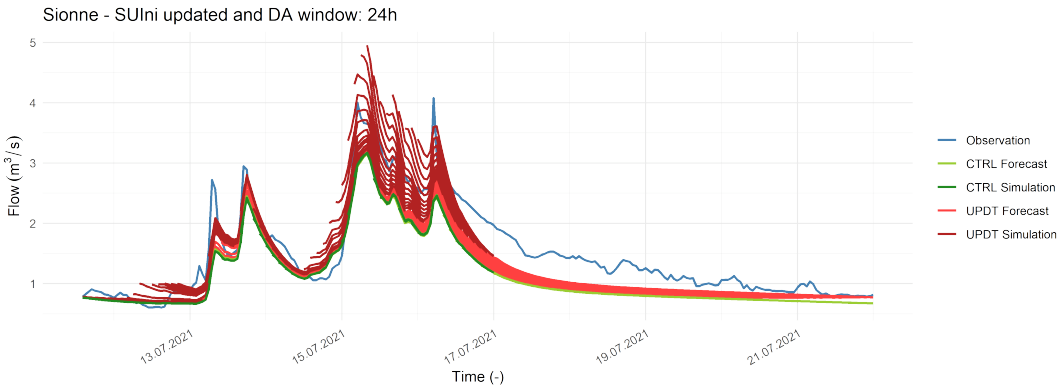

Figure 30 – Results after attempting to update the SU variable for the Sionne watershed, example of the July 2021 event.

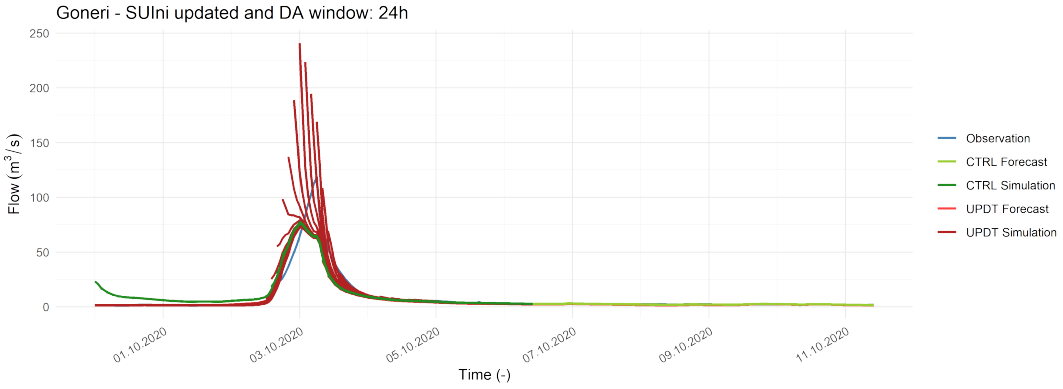

Figure 31 – Results after attempting to update the SU variable for the Goneri watershed, example of the October 2020 event.

C.2 Forecast variability with Hum variant

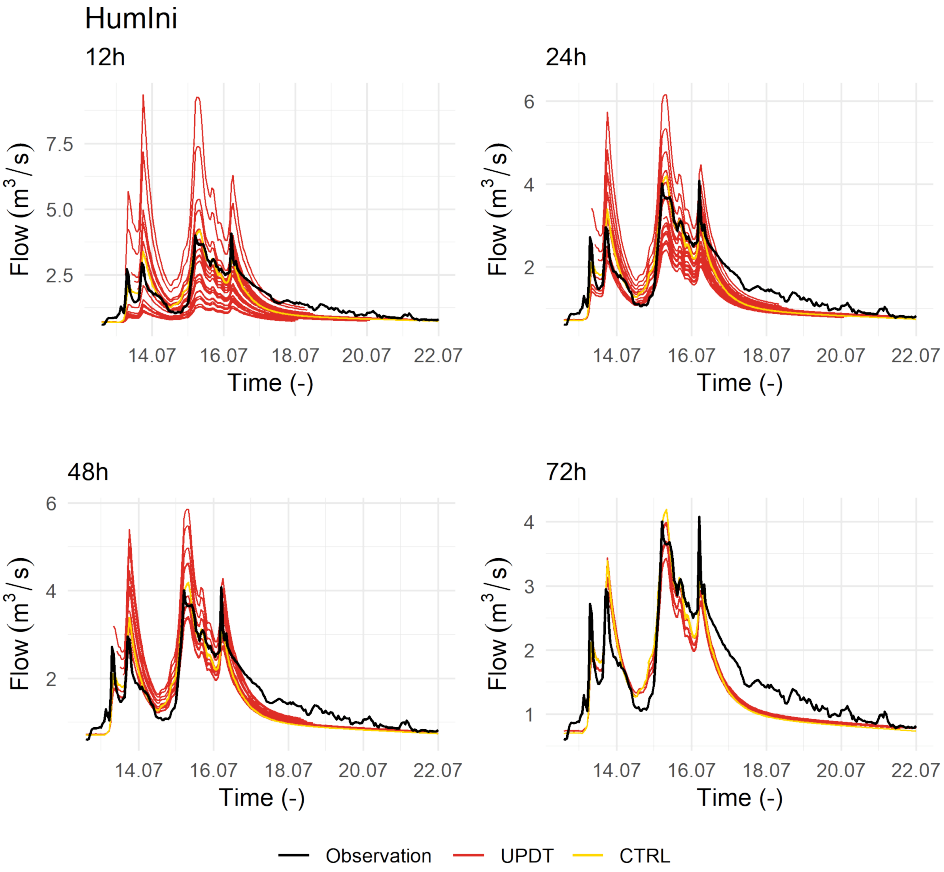

Figure 32 – Variability of hydrological forecasts according to the assimilation window length when updating the Hum variable for the Sionne watershed, example of the July 2021 event.

C.3 Reassessment of flow measurements by the FOEN in December 2021

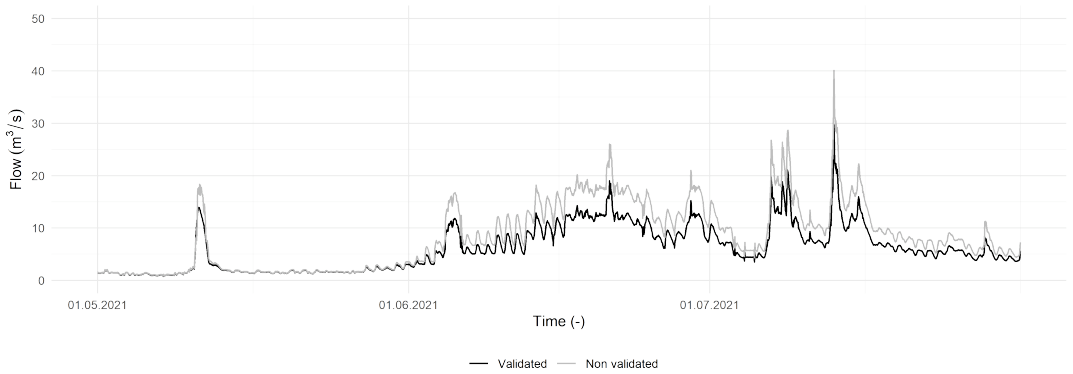

(a)

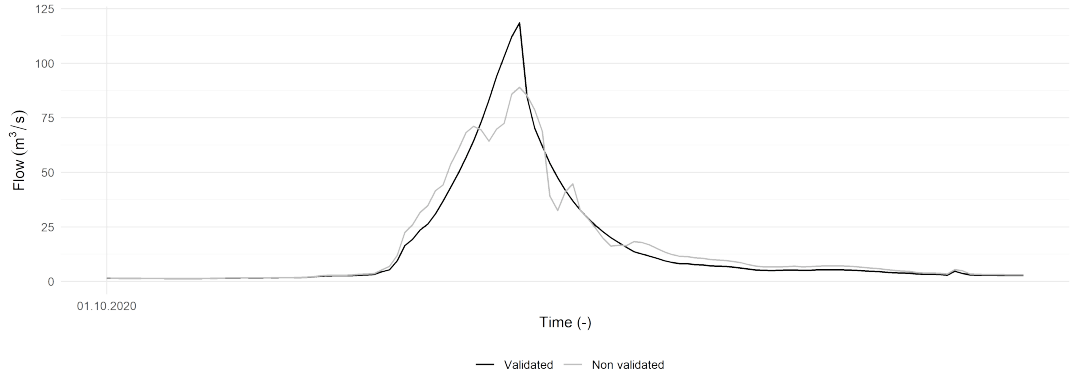

(b)

Figure 33 – Flow differences between the values validated by the FOEN and the real time data initially received (non-validated data).

C.4 Sionne: distribution of SL and Hum variables for each elevation band over 4 years simulation.

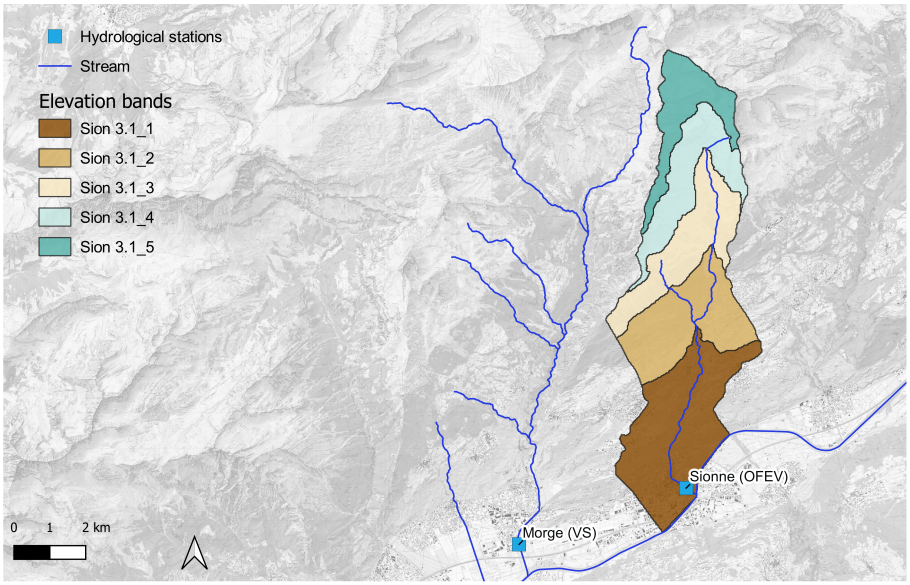

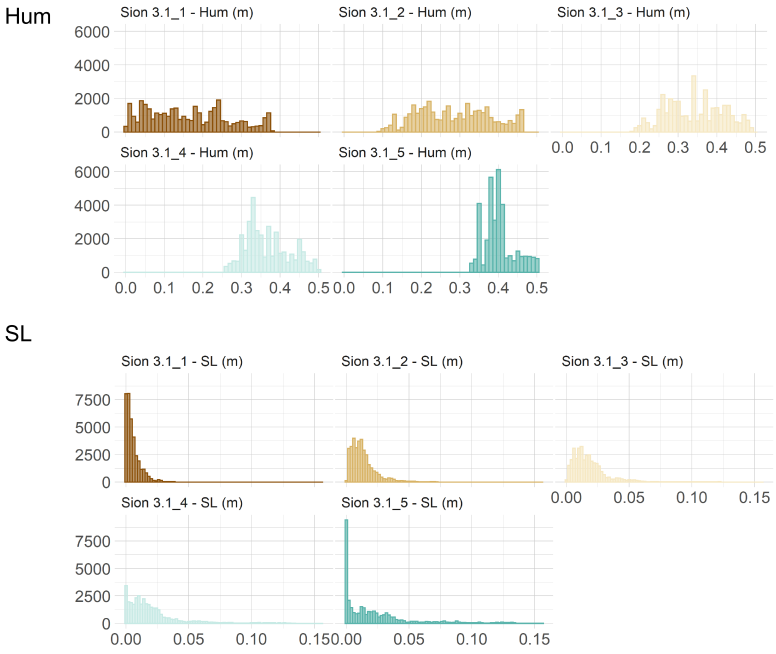

C.5 Goneri: distribution of SL and Hum variables for each elevation band over 4 years simulation.